Development in the European flounder (*Platichthys flesus*) of a q-PCR assay for the measurement of telomere length, a potential biomarker of pollutant effects for biomonitoring studies

Akcha Farida [1, *], Cahuc C. [1], Rouxe Julien [1], Munschy Catherine [1], Aminot Yann [1], Chouvelon Tiphaine [1], Mahe Kelig [2], Budzinski H. [3], Mauffret Aourell [1]

[1] Ifremer, Biogeochemistry and Ecotoxicology Research Unit, Nantes, France
[2] Ifremer, Laboratory of Fisheries Resources, Boulogne-Sur-Mer, France
[3] UMR CNRS 5805 EPOC, Laboratory of Physico- and Toxico-Chemistry of the Environment, Bordeaux, France

* Corresponding author : Farida Akcha, email address : Farida.Akcha@ifremer.fr

Abstract :

Telomeres protect the coding sequence of chromosome ends and Telomere Length (TL) has been proposed as a biomarker of cellular aging, cumulative stress exposure and life-span in humans. With the aim to propose new biomarkers, a q-PCR protocol was adapted for the measurement of TL in the European flounder Platichthys flesus. The protocol was then applied in 2-year-old flounders from the Seine Estuary.

The absolute TL in the flounder is 54 ± 13 kbp per genome (mean ± standard error). Considering relative or absolute TL, no correlation was observed with DNA damage and any of the measured contaminant concentrations (trace elements, metabolites of polycyclic aromatic hydrocarbons, polychlorobiphenyls, organochlorinated pesticides, polybrominated diphenyl ethers, perfluoroalkyl substances). Because sampling was limited, further investigations are required to state a possible impact of chemical pollution on flatfish telomeres. This is motivated by correlations observed with organochlorinated compounds when decreasing statistical significance (p ≤ 0.10).

Highlights

► A q-PCR protocol was adapted for telomere length (TL) measurement in flounders. ► In fish from Seine Estuary, the absolute TL is 55 ± 12.8 kbp per diploid genome. ► No correlation between TL and DNA damage was observed. ► TL is positively correlated with organochlorinated compounds for *p*-values ≤0.10. ► More studies are required to state if TL could be a marker of chemical stress.

Keywords : Flatfish, Pollution, Biomonitoring, Telomere, Genotoxicity, DNA damage

1. Introduction

Estuarine and coastal marine systems are some of the most fertile ecosystems. They are, however, exposed to high anthropic pressures, receiving complex mixtures of chemical contaminants from multiple point and non-point sources. In addition to historical chemical contaminants, such as polycyclic aromatic hydrocarbons (PAHs) and polychlorobiphenyls (PCBs), in the last decades, the presence of contaminants of emerging concern (CECs) has attracted growing interest due to the risk they represent for human and environmental health (Lei et al., 2015). The transfer of chemical substances is particularly important along the land-sea continuum. Chemical pollution represents a risk to the biodiversity and the functioning of marine ecosystems. Following absorption and, in some cases, biotransformation, chemical pollutants can in fact be responsible for various adverse biological effects.

Chemical pollution of aquatic ecosystems raises important environmental, sanitary and socio-economic issues, and an increased awareness has led to changes in European water policies. The Water Framework Directive (2000/60/EC and 2013/39/EC) and the Marine Strategy Framework Directive (MSFD 2008/56/EC) aim to achieve a good quality status in member states' water bodies, in particular by reducing their chemical contamination. Within the MSFD, the anthropic pressure is evaluated by the assessment of 11 descriptors, of which Descriptor 8 (D8) "Concentrations of contaminants are at levels not giving rise to pollution effects" especially addresses chemical pollution effects. In France, the application of MSFD for D8 has led to the implementation of monitoring programmes in the various marine sub-regions concerned by the metropolitan limits of French marine territory. A list of chemical contaminants to be measured in abiotic and biotic matrices has been established, including several trace elements (Ag, As, Cd, Co, Cr, Cu, Fe, Hg, Mn, Mo, Ni, Pb, Zn) and organic contaminants (PAHs, PCBs, organochlorinated pesticides (OCPs), polybrominated diphenyl ethers (PBDEs) and perfluoroalkyl substances (PFASs)). In addition, pollutant effects are studied by measuring several biomarkers in marine organisms (e.g. DNA strand breaks, acetylcholinesterase activity and lysosomal membrane stability in fish and bivalves). Since 2015, different sites in France have been monitored, including the highly anthropised Seine Estuary.

In ecotoxicology, damages to the genetic material are particularly studied. Genotoxicity is a kind of toxicity shared by a high number of pollutant families, occurring at low exposure levels. It can lead to negative health effects such as those observed on embryo-larval development and reproduction in bivalve molluscs and crustaceans (Wessel et al., 2007, Lacaze et al., 2011). Moreover, damage can be transmitted over generations, leading to multi-and trans-generational effects (Barranger et al., 2014). Among pollutant-induced DNA lesions, DNA adducts, DNA strand breaks and micronuclei have been

63 widely measured as genotoxicity biomarkers in sentinel flatfish species such as the European flounder,

64 *Platichthys flesus* (Akcha et al. 2003, Hylland 2017). In the Seine Estuary, their measurement in dab

65 *Limanda limanda* showed evidence for fish exposure to genotoxic pollutants such as PAHs (Akcha et

66 al., 2003, 2004, Devier et al., 2013). These genotoxicity biomarkers are on the list of endpoints

67 proposed by the International Council for the Exploration of the Sea (ICES) for an integrated framework

68 to assess chemical pollution in the marine environment.

69 With the aim to pursue the development of genotoxicity biomarkers, it appeared valuable to

70 investigate the impact of chemical pollution on a part of the chromosome structure, the telomeres, in

71 flatfish, poorly investigated until now in ecotoxicology. Telomeres play a key role in maintaining

72 genomic stability by protecting the coding sequence of chromosome ends (Monaghan et al., 2018).

73 Highly conserved across eukaryotes, telomeres are made of tandem repeat of a non-coding short

74 hexameric DNA sequence (TTAGGG). They range from a few to 15 kb in length in humans (Barnes et

75 al., 2019), being even higher (> 30 kp) in several vertebrate animal species (Whittemore et al., 2019).

76 Because of the impossibility to complete DNA replication up to chromosome ends and semi-

77 conservative replication of the DNA, at each cell division, a portion of telomeres is not replicated, and

78 therefore, they are naturally shortened during aging. In humans, telomere length (TL) has been

79 proposed as a potential biomarker of cellular aging and cumulative stress exposure, as well as a

80 prognostic indicator for risk of late-life diseases (Von Zglinicki, 2002). In the last decades, several

81 epidemiology and toxicology studies have highlighted a disruption of telomere dynamics during

82 exposure to oxidative stress as well as physical and chemical agents (Barnes et al., 2018, Moller et al.

83 2018).

84 This seems to be also the case in animals such as birds. In a previous *in-situ* study on the relationship

85 between contaminant exposure and TL in the black-legged kittiwake *Rissa tridactyla* different findings

86 were obtained. In adult females, the TL of red blood cells (RBCs) was negatively correlated with the

87 concentration of an organochlorine pesticide, namely oxychlordane, in the blood (Blévin et al., 2016).

88 In contrast, a positive and significant relationship was observed between PFAS concentration and

89 telomere dynamics in birds presenting higher levels of contamination (Blévin et al., 2017). In fish, a

90 study conducted in the gold fish *Carassius auratus* showed an increase in the level of DNA strand breaks

91 in telomeric regions following exposure to the organophosphorus pesticide monocrotophos,

92 suggesting a potential impact on their length (Zhao et al., 2015). Very recently, shorter telomeres were

93 associated with high levels of phthalate metabolites in the European chub *Squalius cephalus* from

94 urban and agricultural rivers (Molbert et al., 2021). Knowledge on telomeres dynamics in fish is limited;

95 TL length varies from 2 to 25 kb, depending on the species (Ocalewicz, 2013). Unlike in humans,

96 telomerase in fish can be expressed in most tissues throughout the life of the organism (Horn et al.,

97 2008), and a decrease in length over the course of life has not been verified in all fish species (Simide

98 et al., 2016).

99 In the present study, a q-PCR (quantitative Polymerase Chain Reaction) protocol was adapted from

100 O'Callaghan et al. (2008) for the measurement of relative and absolute TL in the blood of flounders.

101 The protocol was developed and validated using a composite DNA sample from fish sampled in the

102 Seine Estuary. To start investigating a possible link between pollution and genome integrity in marine

103 flatfish, it was then applied in individuals from the same ontogenetic stage. The relationship between

104 TL, DNA damage (level of DNA strand breaks in the erythrocytes) and chemical body burden (biliary

105 PAH metabolites, hepatic concentrations in several trace metal elements and muscle concentrations

106 of mercury, PCBs, PBDEs, OCPs and PFCAS) was investigated.

107

108 **2. Material and methods**

109 **2.1 Chemicals**

110 We purchased NaCl, trizma base, dimethyl sulfoxide (DMSO), normal and low-melting-point agarose,

111 Triton X-100, foetal calf serum and GelRed from Sigma Aldrich Chemicals. The DNeasy®- Blood and

112 Tissue kit was obtained from Qiagen, and *E. coli* pUC 19 plasmid, DH5alpha *Escherichia coli* bacteria,

113 SOC medium, Luria Broth medium and ampicillin were purchased from Thermo fisher Scientific.

114 PureLink Quick Plasmid DNA Miniprep Kits, purifying DNA with a centrifuge, were obtained from

115 Invitrogen. Brilliant III Ultra-fast SYBR Green QPCR Master Mix and ROX were purchased from Agilent.

116 Custom primers and oligomers (84-mer telomeric oligomer and 76-mer GAPDH oligomer) were

117 synthetised by Eurogentec. Contaminant analyses were conducted using carefully chosen chemicals

118 selected to satisfy trace analysis requirements. Details can be found in Munschy et al. (2020a) for

119 organic contaminant analyses in fish tissue. The hydroxy-PAHs and their deuterated homologs were

120 obtained from Cambridge Isotope Laboratories (Cluzeau Info Labo, Sainte Foy la Grande, France). All

121 the standards were of analytical grade (> 98%). All the solvents used were of analytical grade (purity >

122 98%). Dichloromethane and HPLC grade methanol were obtained from Atlantic Labo (Bruges, France).

123 Deionised water was obtained with a Milli-Q system from Millipore (Molsheim, France).

124

125 **2.2 Sampling**

126 Fish were collected in the Seine Estuary, which is located in the Eastern Channel (Figure 1). It is the

127 third-largest French estuary (Flipo et al., 2020). It accounts for 50% of the French river transport, and

128 its catchment area supports 40% of the French economic activity. It is considered to be one of the most

129 polluted estuaries in Europe (Tappin and Millward, 2015, Burgeot et al., 2017), affected by both large

130 urban centres (e.g. Paris and its suburbs), wastewater treatment plants, intense industrial (e.g. harbour

4

and petrochemical activities) and agricultural (mass production of cereal and industrial crops) activities. Nutrients and several contaminants from urban, industrial and agricultural activities are thus discharged into the English Channel by the Seine, the main river flow into the Channel. Species living in the Seine Estuary and the Seine Bay are thus exposed to cocktails of contaminants.

Flounders were caught in September 2018 by trawling on the R/V Antéa in the Seine Bay. The sampling was performed during the SELISEINE survey (https://doi.org/10.17600/18000585), which is part of the national monitoring survey of the chemical effect (SELI: https://doi.org/10.18142/285). The Seine Bay has been previously studied for biomonitoring surveys using dab (Akcha et al. 2003, 2004, Munschy et al. 2004). For the present study, we focused on a sampling area close to the mouth of the Seine Estuary and consequently exposed to the Seine River plume, which carries diverse chemical contaminants.

Fish were collected with a small-mesh bottom trawl net. Trawling was limited to 20 min at a speed of 3 knots to allow live fish recovery. Only fish having a total length of around 25 cm were selected. This fish length corresponds to 2–3-year-old individuals that are sexually mature (Drevs et al., 1999, van der Hammen and Poos, 2012). They were kept alive on board in a fish well and dissected at the quay. A total amount of 22 fish was available for the study.

2.3 Biometry, collection and storage conditions of individual fish blood, tissues and otoliths

Back to the dock (between 2 and 8 h after fishing), individuals were measured (total length, to the nearest tenth of a cm) and weighed before blood was sampled directly from the caudal vein, using a heparinised syringe. An average of 100 µL of blood was recovered in a cryotube containing RPMI 1640 medium supplemented with foetal calf serum (25%) and dimethyl sulfoxide (DMSO; 20%) and stored in liquid nitrogen prior to analysis by the alkaline comet assay for the measurement of DNA stand breaks. The rest was used to isolate total blood cells by centrifugation before storage in liquid nitrogen; these samples were used for the methodological development for TL measurement by q-PCR. Fish were then sacrificed for dissection.

Macroscopic observation of the gonads allowed sex determination. The gall bladder was sampled individually for the measurement of biliary hydroxylated PAH metabolites (3-OH BaP, 9-OH BaP, 3-OH Fluo, 1-OH Pyr). The liver was stored below 20°C in acid-cleaned glass vials for trace metal analysis (refer to 2.8). The eviscerated fish was then weighted and saved in a calcined aluminium foil at -20°C prior to dissection of fish muscle under a laboratory hood for subsequent analysis of organic contaminants (PCBs, PBDEs, HBCDDs, OCPs, PFASs) (refer to 2.9) and mercury analysis on this tissue (refer to 2.8). At this final time, sagittal otoliths were collected from the inner ear of each fish (Figure 2), cleaned with distilled water and stored at room temperature.

165
1
2 166
3
4
5 168
6
7 169
8
9
10 171
11
12 172
13
14 173
15
16 174
17
18 175
19
20
21 177
22
23 178
24
25 179
26
27
28 181
29
30 182
31
32 183
33
34 184
35
36 185
37
38 186
39
40
41 188
42
43 189
44
45 190
46
47
48 192
49
50
51 194
52
53 195
54
55 196
56
57 197
58
59 198
60
61 199
62
63
64
65

2.4 Otolith sclerochronology

166 An otolithometric approach was used to determine the age of the 22 flounders according to the

167 international ageing protocol (Vitale et al., 2019). Otoliths (literally 'earstones') are paired, calcified

168 pieces of the inner ear of teleosts, growing continuously during fish life and forming annual increments

169 (Panfili et al., 2002). The otolith shape is species-dependent, and for this reason, the ageing

170 preparation could be different among different flatfish species. For flounder, the whole otolith was

171 used. All otoliths were photographed using a ZEISS microscope under transmitted light, assisted by an

172 image analysis system using the TNPC software for digital processing of calcified structures. These

173 calibrated images showed an alternate succession of translucent and opaque bands. It was assumed

174 that the growth annual ring (named "annulus") consisted of one opaque and one translucent band.

175 Two readers to limit the bias due to ageing analysed each otolith (Vitale et al., 2019).

176

2.5 Development of a q-PCR protocol for the measurement of absolute and relative TL in the

European flounder

179 2.5.1 Methodological principles

180 It is noteworthy that due to important chromosomal rearrangements over the course of evolution,

181 some flatfish species may have also telomeres in the body of the chromosomes, so-called "ITS"

182 (interstitial telomere sequences), which are mostly shorter than telomeres (Bitencourt et al., 2014).

183 Because the Senegalese sole *Solea senegalensis* and the Atlantic halibut *Hippoglossus hippoglossus* are

184 ITS-free (Ocalewicz et al., 2008 and Cross et al., 2006), this is expected to be also the case in the

185 flounder, which belongs to the same phylogenetic *Pleuronectidae* family. Therefore, there is no risk of

186 underestimating telomere length in these sentinel species due to the presence of ITS (Foote et al.,

187 2013).

188 The use of the Terminal Restriction Fragment (TRF) is the reference method to measure TL (Harley et

189 al., 1990). Because it requires less DNA quantity, q-PCR was first used by Cawthon et al. (2002) to

190 measure the relative TL in human RBCs by establishing the ratio between the cycle threshold value (Ct)

191 of the telomeric sequence (T) and those of a single-copy reference gene (S). The q-PCR has been widely

192 applied, and in 2008, O'Callaghan et al. proposed an advanced q-PCR protocol for the measurement of

193 both relative and absolute TL. The authors generated an external calibration curve based on the

194 amplification of known quantities of a telomeric oligomer of a known base pair number. A similar

195 calibration curve was also obtained for a single-copy reference gene to allow the determination of the

196 number of genome copies present in the samples. With these curves, it was thus possible to give a

197 value for absolute TL in kilobase pair (kbp) per unit of genome present in each sample subjected to

198 amplification.

199

6

200   2.5.2 DNA extraction

201   The DNA was extracted from flounder blood cells using the DNeasy®-Blood and Tissue kit, following

202   the recommendations of the manufacturer. Once extracted, DNA concentration and quality were

203   measured by spectrophotometry at 230, 260 and 280 nm, using a Nanodrop ND1000. The DNA samples

204   presenting 260/280 and 260/230 ratios, around 1.8 and 2, respectively, were considered as pure. For

205   the quantification, one optic density unit at 260 nm corresponded to a concentration of 50 µg pure

206   DNA per mL.

207

208   2.5.3 Plasmid DNA extraction

209   For TL measurement by qPCR, it is recommended to maintain the initial DNA quantity constant for the

210   establishment of standard calibration curves (O'Callaghan et al., 2008). To do so, plasmid DNA deprived

211   of the telomeric sequence was used. First, 2 µL of *E. coli* pUC 19 plasmid were added to 100 µL of

212   DH5alpha *E. coli* bacteria, and plasmid insertion was realised by thermal shock (30 s at 42°C, followed

213   by a rapid switch into the ice to tighten pores and to entrap plasmids inside the cells). Bacteria were

214   then incubated with SOC medium (tryptone 2%, yeast extract 0,5%, NaCl 10mM, KCl 2,5 mM, $MgCl_2$

215   10mM, $MgSO_4$ 10 mM, glucose 20mM) for at least 30 min to allow cell transformation. Subsequently,

216   they were cultured in a petri dish containing ampicillin-enriched Luria Broth (LB) medium for 24 hrs at

217   37°C. In these conditions, only bacteria with inserted plasmid DNA expressed the ampicillin resistance

218   trait phenotype. Those bacteria were then recovered and suspended in ampicillin-enriched LB medium

219   for 24 h at 37°C prior to DNA extraction using the "Pure Link Quick Plasmid DNA Miniprep Kits- Purifying

220   DNA with a centrifuge", following the manufacturer's instructions. Plasmid DNA concentration and

221   quality were determined as previously described.

222

223   2.5.4 q-PCR assay

224   We performed q-PCR using the Brilliant III Ultra-fast SYBR Green QPCR Master Mix kit, following the

225   manufacturer's instructions. The adaptation of the protocol from O'Callaghan et al. (2018) was realised

226   using a composite DNA sample made of genetic material from the different fish caught at ES station.

227   The use of a kit was not conducive to modifications on Taq polymerase quantity and composition and

228   quantity of the reaction buffer. Four parameters of the qPCR procedure were tested to optimise

229   sensibility and specificity of the telomere length measurement in flounder: the quantity of amplified

230   DNA (7.8×10^{-2} to 5 ng), the primer set (refer to 2.6.4.1), the hybridisation temperature (54 to 60°C)

231   and the ratio of forward and reverse primers (1 to 3); those values were chosen according either to

232   previous published protocols (Cawthron et al., 2002, O'Callaghan et al., 2008, Angelier et al.,2013) or

233   to the manufacturer's recommendations.

234 The q-PCR conditions were validated for PCR efficiencies ($E = 10^{(-1/slope)} - 1$) of 100% (± 10%) and

235 following an examination of the dissociation curves to check for PCR specificity. An agarose gel was

236 also used to verify the number and size of amplification products. All assays were conducted with

237 respect to the Minimum Information for Publication of Quantitative Real-Time PCR Experiments

238 (MIQE) Guidelines, published by Bustin et al. (2009).

239

240   2.5.4.1 Primers for reference genes and telomere sequence

241 Different primer sets were designed for the reference gene and the telomeric sequence, using the

242 Primer3 software (web version 4.1.0 from Whitehead Institute for Biomedical Research). The primer

243 design for the reference gene was based on gene sequences already published and available from the

244 National Centre for Biotechnology Information (NCBI). For the flounder, glyceraldehyde-3-phosphate

245 dehydrogenase (GAPDH) was selected as the reference gene for which different sets of primers were

246 designed with respect to the q-PCR kit manufacturer's recommendations (hybridisation temperature

247 of 60°C, 20 base pairs in length). Primers were then synthetized and stored at a final concentration of

248 100 µM in molecular biology grade water at -20°C prior to use for amplification tests. Concerning the

249 telomeric sequence, we tested the primers suggested by O'Callaghan et al. (2008).

250 Different assays were performed. Following several adjustments, amplifications were optimal for the

251 primer sets and concentrations presented in Table 1. The annealing temperature was optimal for all

252 assays at 60°C.

253

254   2.5.4.2 Generation of standard curves

255 For absolute telomere length measurement, a calibration curve was obtained by using a telomeric

256 oligomer (84-mer) corresponding to 14 tandem repeats of the hexameric telomeric scheme

257 (TTAGGGTTAGGGTTAGGGTTAGGGTTAGGGTTAGGGTTAGGGTTAGGGTTAGGGTTAGGGTTAGGGTTAGG

258 GTTAGGGTTAGGG). A similar curve was also obtained for the selected reference gene, using as

259 oligomer the amplification product obtained with the selected primer set. The 76-mer GAPDH oligomer

260 had   the   following   sequence: CCTGCCGTCACTG

261 GGATTACCACAGTGGGAGGCTCATTTCGACTTTGACCCCCAGAGAGGAGAGTGGGAGAGCTGT.

262 Standard curves were generated by the q-PCR amplification of serial dilutions (10^{-1} to 10^{-6}) of the target

263 oligomer, corresponding to an initial DNA quantity ranging from 6 fg to 60 pg per reaction for the

264 telomeric oligomer and from 2 fg to 20 pg per reaction for the single-copy gene. Because the initial

265 DNA quantity was optimum for 1 ng per reaction, it was maintained constant by the addition of plasmid

266 DNA. For each point of the curve, reactions were performed in triplicates.

267

268   2.5.4.3 q-PCR conditions for standard curves and fish sample analysis

269 The q-PCR assays were run using the Stratagene MX3000P instrument with the Stratagene MXPro

270 software. Telomere and GAPDH were amplified for each fish sample on two different polypropylene

271 96-well tube plates. On each plate, the corresponding oligomer was also run to generate the external

272 calibration curve. A No Template Control (water and reaction mix only) and a composite sample of fish

273 DNA were also analysed on each plate to check for contamination and inter-plate variation,

274 respectively.

275 The QPCR Master Mix contained the mutant Taq DNA polymerase, dNTPs, Mg^{2+}, a buffer specially

276 formulated for fast cycling and the double-stranded DNA-binding dye SYBR Green I for detection

277 (excitation and emission wavelengths of 254 and 520 nm, respectively). The forward and reverse

278 primers (see 2.6.3.1) and a reference dye (ROX at 1:500, 30 nM) were then added into the mix and

279 gently mixed. The passive reference dye is included in the kit to compensate for non-PCR-related

280 variations in fluorescence, providing a stable baseline to which samples are normalised (excitation and

281 emission wavelengths of 584 and 612 nm, respectively). After distributing the mix in the plate's well,

282 1 ng of DNA was added per reaction (plasmid DNA was used to maintain the amount constant); the

283 final total reaction volume was 20 µL. The plate was then homogenised and centrifuged. For both

284 telomeres and single-copy gene, PCR conditions were as follows: 3 min at 95°C (Taq activation), 40

285 cycles of 20s at 95°C, followed by 20s at 60°C (denaturation of dsDNA template followed by annealing

286 and extension of the primers), 95°C for one min, 30s at 55°C, 30s at 95°C (dissociation step). Regarding

287 the calibration point, each fish sample was run in triplicate, and some samples were run a second time

288 when the difference in Ct values among the triplicates was greater than 1 Ct.

289

290   2.5.4.4 Calculation of relative and absolute TL

291 The relative TL was determined as described by Cawthon et al. (2002) by the ratio between the Ct value

292 of the telomeric sequence (T) and that of a single-copy reference gene (S).

293 The absolute TL was determined based on the calibration curves obtained for the telomeric sequence

294 and the reference gene, as described by O'Callaghan et al. (2008). The oligomer standard for the

295 telomeres has a molecular weight (MW) of 26,667.2

296 (http://biotools.nubic.northwestern.edu/OligoCalc.html). The weight of one molecule (the Avogadro's

297 number gives the number of units in a mole) was therefore 0.44×10^{-19}g for a 84-mer length. For each

298 amplified quantity of the oligomer standard, it is therefore possible to assign a number of total

299 amplified TL in kilobase pairs to each Ct value. Concerning the reference gene, the weight of one

300 amplicon molecule was calculated (MW/Avogadro's number) and used to determine the number of

301 diploid genome copies present in amplified DNA (quantity of standard divided by the amplicon weight

302 and then by 2 to take into account diploidy). By using these calibration curves, the absolute TL of each

303 fish DNA sample was determined and expressed in kbp/diploid genome.

9

2.6 Investigating *in situ* the relationship between chemical pollution and genome integrity in flounder

Because age can have an influence on TL, it was decided to focus on 2-year-old fish, representing most of the fish collected at ES during the survey (see 3.1). TL, DNA damage and complete chemical analysis were conducted on the same set of samples made of 8 fish (4 males and 4 females).

2.6.1 Measurement of DNA strand breaks in fish erythrocytes

The comet assay was applied as previously described (Akcha et al., 2003). Two comet slides were prepared per blood sample; DNA unwinding and electrophoresis (390 mA, E = 0.66 V cm^{-1}) duration were, respectively, 15 and 20 min. To obtain permanent preparations, the slides were immersed for 10 min in absolute ethanol for dehydrating and allowed to dry at room temperature. Immediately prior to analysis, 75 µL of GelRed at 8 mg L^{-1} were spread over each slide using a cover glass. The slides were placed for at least 1 h in the dark at 4°C for coloration and then analysed using an optical fluorescence microscope (Olympus BX60 × 40) equipped with a CDD camera (Luca-S, Andor Technology) and an image analysis system (Komet 6, Kinetic Imaging Ltd). At least 50 nuclei were analysed per slide, and the percentage of DNA present in the comet tail (% tail DNA) was measured for each observed nucleus.

2.6.2 Biliary PAH metabolites

The analytical procedure used to quantify PAH metabolites (OH-naphthalenes, OH-phenanthrenes, OH-pyrene, OH-benzo(a)pyrene) was adapted from Mazéas and Budzinski (2005) and Wessel et al. (2013) . Bile samples (10-50 µL) are homogenised with 2 mL of acetate buffer pH5. After adding an internal calibration solution (1-OH-Pyrene-d9 and 4-OH-Biphenyl-d9), an enzymatic deconjugation step is performed at 37°C for 18 hours (β-glucuronidase from Helix pomatia type HP2 and 2-mercaptoethanol). After deconjugation, the bile samples are extracted by solid phase extraction (SPE, C18 cartridge 500 mg 3 mL). The organic extracts were eluted with 2 x 2 mL of methanol, concentrated under gas flow at 50 µL and then re-dissolved in 1 mL of 80/20, v/v dichloromethane/methanol mixture. The resulting extract were purified by solid phase extraction (SPE, NH2 cartridge, 500 mg, 3 mL), eluted with 2 x 2.5 mL of an 80/20, v/v dichloromethane/methanol mixture and concentrated under gas flow at 100 µL in methanol. Finally, the extracts were stored at -20°C until injection. Mono-hydroxylated PAH metabolites were analyzed by LC/MSMS in negative ionization mode (Infinity 1290 LC/6460 Triple Quad LC/MS, Agilent Technologies). The column used for analysis was an Acquity UPLC BEH C18 (1.7 µm x 2.1 mm x 50 mm, Waters), the temperature of the column was set at 45°C. The

injected volume of organic extract was fixed at 5 µL. The gradient of elution solvents was: ultra-pure water/methanol (70/30) to methanol (100%) at 0.6 ml/min (6.5 min). Metabolites were quantified by isotopic dilution in MRM mode. Various quality controls were carried out to validate the analytical procedure. Protocol blanks were carried out in order to verify the absence of cross-contamination during the laboratory sample processing process. The quantification limits and yields were carried out by using spiked model matrix. Quantification limits were characterized and ranged from 1 to 3 ng g^{-1} of bile depending the compounds. Recoveries ranged from 75 to 105% with mean variability of 20%.

2.6.3 Tissue content in trace metal elements

For both metal and organic contaminant analyses, tissues were freeze-dried and ground into a fine powder. All contaminant concentrations are given in dry weight (dw).

In fish muscle, total mercury (Hg) concentrations were assessed by atomic absorption spectrophotometry on aliquots of homogenised powder (~ 40 ± 10 mg), using an Advanced Mercury Analyser (ALTEC AMA-254, Altec Ltd) and according to the standard operating procedure described in the US-EPA method N°7473 (U.S. Environmental Protection Agency, 1998). With this method, the limit of quantification (LOQ) for Hg determination in muscle was 0.015 mg kg^{-1} dw.

In fish liver, total silver (Ag), arsenic (As), cadmium (Cd), cobalt (Co), copper (Cu), iron (Fe), mercury (Hg), manganese (Mn), molybdenum (Mo), lead (Pb) and zinc (Zn) concentrations were determined with a Quadrupole Inductively-Coupled Plasma Mass Spectrometer (Q-ICP-MS, ICAP-Qc model from ThermoFisher), according to an in-laboratory approved method. Briefly, with this method, aliquots of samples (~200 mg of homogenised powder) are placed in Teflon bombs and mineralised with a mixture of ultrapure HNO_3 acid and milli-Q water, using a microwave (ETHOS-UP model from Milestone). The digests are then diluted to 50 mL with milli-Q water before analyses with Q-ICP-MS. With this method, LOQs (in mg kg^{-1} dw) were 0.07 for Ag, Cd, Mo and Pb, 0.86 for As, 0.01 for Co, 0.93 for Cu, 8.6 for Fe, 0.06 for Hg, 0.69 for Mn and 9.3 for Zn.

The quality assurance of all metal analyses relied on blank and internal standard controls and on the accuracy and reproducibility of data relative to the certified reference materials (CRMs) used in analytical runs. The CRMs used were IAEA-407 (whole-fish homogenate; International Atomic Energy Agency/IAEA) and IAEA-142 (mussel homogenate; IAEA) for Hg, as well as DORM-4 (fish protein, National Research Council Canada/NRCC), DOLT-5 (dogfish liver, NRCC) and CE-278k (mussel tissue, Joint Research Centre- European Commission) for the other trace metal elements. Blank values were systematically below the detection limits, and CRM values concurred with certified concentrations, with recovery rates ranging between 88 and 114% for all elements and CRMs.

11

2.6.4 Organic contaminant analysis in fish muscle

Detailed analytical procedures and QA/QC parameters for PCBs, OCPs, PBDEs and PFASs can be found in Munschy et al. (2020b) and references therein. Method precision calculated as the relative standard deviation of replicates was 2-17% for PCBs, 6-28% for OCP, 4-20% for PBDEs and 12-33% for PFASs

For PCBs (i.e. the 7 ICES priority congeners, namely CB-28, -52, -101, -118, -138, -153, -180), OCPs (five dichlorodiphenyltrichloroethane (DDT) isomers, four hexachlorocyclohexane (HCH) isomers and dieldrin) and PBDEs (8 congeners, namely BDE-28, -47, -49, -99, -100, -153, -154, -183), 5 g of freeze-dried sample were extracted by pressurised liquid extraction with dichloromethane. Prior to extraction, $^{13}C_{12}$-labelled compounds were added to the sample for internal standard calibration and quantification using the isotopic dilution method. The extracts were successively purified using gel permeation chromatography, a silica and alumina adsorption chromatography column and a two-dimensional HPLC system with two columns coupled in series. Analyses were performed by gas chromatography coupled to a high-resolution mass spectrometry (GC–HRMS), using a Hewlett-Packard 6890 gas chromatograph coupled to an AutoSpec Ultima mass spectrometer (Waters Corp.).

For PFASs, 1 gram of a freeze-dried sample, to which an internal standard mixture of nine labelled compounds was added prior to agitation, was extracted using liquid-solid extraction with MeOH/KOH (0.01 M of KOH), purified onto two consecutive SPE cartridges (a weak anion exchange (WAX) stationary phase and a graphite (Envicarb) stationary phase), evaporated to dryness and reconstituted in 200 μL of a mixture of MeOH/H_2O (50/50, v/v), containing the injection standard, PFOS $^{13}C_8$. Targeted analytes (including C_4- to C_{10}-perfluoroalkyl sulfonates (PFSAs) and C_6- to C_{14} perfluorocarboxylic acids (PFCAs)) were quantified using the corresponding isotope-labelled standard. Analysis was performed using an Acquity ultra-performance liquid chromatograph (UPLC®, Waters Corp.) coupled to a triple quadrupole mass spectrometer (Xevo® TQ-S micro, Waters Corp.) interfaced with a Z-spray™ (Waters Corp.) electrospray ionisation source.

2.10 Statistical analysis

Means were always given with their respective standard error. Regression analysis were performed using the software package Statistica 8.0 (General regression models, Pearson correlation coefficient). The effect of sex on both TLs and DNA damage (4 males and 4 females) was studied by applying nonparametric Mann-Whitney U tests (Statistica Soft. 8.0). Significant differences were considered at $p < 0.05$.

3. Results

3.1 Age and sex distribution of flounders caught at ES station

The age and sex of the flounders caught during the survey at ES location are given in Figure 3. First, it is noteworthy that for the same length class, age could vary from 1 to 3 years. Otolith analysis showed that 60% of the flounders sampled were 2 years old (67 and 50% males and females, respectively).

3.2. Validation of the QPCR assay for the measurement of TL in the flounder

Regarding the MIQE Guidelines, the PCR efficiencies of the different sets of primers used for the amplification of the telomeric sequence and the single-copy gene using either composite DNA or standard oligomers were all validated, with values between 98 and 104% (Table 2). This is illustrated in Figure 4 for the amplification of the telomeric sequence and the GAPDH gene in the composite DNA sample. For the telomere and GAPDH oligomers, standard curves were obtained to allow absolute TL measurement (Figure 5).

TL data are presented only for 2-year-old flounders (see 3.3) as the number of fish from the other age classes was insufficient.

3.3 TLs and level of DNA damage in 2-year-old flounders from the Seine Bay

The relative and absolute TLs were 0.811 ± 0.017 and 54.3 ± 12.8 kbp, respectively (mean ± standard error). Considering the number of chromosomes in the flounder (2N = 48, Saygun, 2015), the mean length of a telomere unit is around 0.57 ± 0.13 kb (mean ± standard error). Relative and absolute TLs were negatively correlated (R^2 = 0.925, p < 0.001) (Figure 6). The longer is the TL and the lower are the corresponding Ct value and T/S ratio. Irrespective of relative or absolute TL, no difference was observed between female and male flounders (Mann Whitney U tests, n = 4 per sex, p = 0.69 and p = 0.34, respectively).

In the erythrocytes, application of the comet assay gave a % tail DNA value of 15.71 ± 3.72 (mean ± standard error), with no difference between fish sex (n = 4 per sex, p = 0.99).

3.4 Chemical contamination of 2-year-old flounders

3.4.1 Tissue concentrations of trace metal elements (TMEs)

The measured concentrations for TMEs in the liver (Ag, As, Cd, Co, Cu, Fe, Hg, Mn, Mo, Pb, Zn) and in the muscle (Hg) are reported in Table 3.

3.4.2 Levels of biliary PAH metabolites

13

433 One- and 2-hydroxy metabolites of naphthalene were detected above the quantification limit in only

434 two individuals (concentrations of 6 ng g^{-1} bile). In contrast, hydroxyl metabolites of phenanthrene

435 were detected in nearly all fish analysed, which the exception of one individual; most of these

436 metabolites (76%) were made of 2-OH and 3-OH. Nine-OH BaP was the only detected BaP metabolite

437 in fish bile, with the exception of one individual (26 ± 10 ng g^{-1}). The major PAH metabolite was 1-OH

438 pyrene (226 ± 78 ng g^{-1} bile), representing more than 80% of the total measured PAH metabolites in

439 fish bile (∑hydroxylated PAH metabolites of 260 ± 90 ng g^{-1} bile).

440 3.4.3 Levels of PCBs, OCPs, PBDEs and PFASs in flounder muscle

441 In all samples, PCB and PBDE congeners, DDT isomers, dieldrin, PFOS and long-chain PFCAs were above

442 the LOQs, while among HCH isomers, δ-HCH was below the LOQ in three out of eight analysed fish.

443 The highest concentrations were found for PCBs (97.2 ± 25.3 ng g^{-1} dw), followed by PFASs (4.85 ± 1.48

444 ng g^{-1} dw), OCPs (2.57 ± 0.66 ng g^{-1} dw) and PBDEs (0.51 ± 0.14 ng g^{-1} dw) (Table 4). Highly significant

445 correlations were found between PCB, OCP, PBDE and PFAS concentrations (R^2 between 0.61 and 0.98,

446 $p < 0.05$).

447 Although the significance of sex-related differences in POP concentrations could not be tested because

448 of a limited number of samples of each sex, no tendency in POP concentrations was observed between

449 male and female individuals. The results were therefore considered for both sexes together.

3.4 Correlations between TLs, DNA damage and chemical contamination in flounders

451 Regardless of considering relative or absolute TL, no correlation was observed with the percentage of

452 tail DNA and any of the chemical contaminants measured in flounder tissue when considering

453 statistical significance from a p-value < 0.05 (Table 5). However, relative TL could be positively

454 correlated to OCPs, DDT and PCBs by increasing the α risk value from 0.05 to 0.10 (e. g. the p-value

455 associated to the coefficient of determination between relative TL and DDT is $0.05 < 0.081 < 0.10$). In

456 this study, the percentage of tail DNA was not correlated with chemical contamination (Table 5).

457 Considering individual trace elements rather than their sum did not change the results, except for Mn

458 and Fe, which were positively correlated to the % tail DNA ($p = 0.021$ and $p = 0.007$, respectively).

459

4. Discussion

4.1 Telomere length is species-specific, and its value can vary depending on the methods used for its measurement

14

463 In the present study, a first measurement of TL by q-PCR was realised in the flounder (mean absolute

464 TL of 54.3 kpb/diploid genome, mean of a telomere unit length of 0.57 kpb). It was possible to compare

465 this result to other published data obtained in fish species using either TRF or the Telomere Amount

466 and Length Assay (TALA) technique. Telomere length varies between fish species when comparing data

467 obtained in the European sea bass *Dicentrarchus labrax* (2.8-4.9 kb, TRF technique, Horn et al., 2008),

468 the killifish *Fundulus heteroclitus* (2.0–10.0 kb, TALA technique, Elmore et al., 2008), the American eel

469 *Anguilla rostrata* (10.0–15.0 kb, TALA technique, Elmore et al., 2008), the rainbow trout *Oncorhynchus*

470 *mykiss* (up to 20 kb, TRF technique, Leijnin et al., 1995), the Japanese medaka *Oryzias latipes* (3.0–12.0

471 kb, TALA technique, Elmore et al., 2008) and the zebrafish *Dana rerio* (2.0–10.0 kb, TALA technique,

472 Elmore et al., 2008). However, comparisons must be done with care, as in recent years, several papers

473 dealt with the different techniques used to measure TL and their respective limitations. Among all the

474 techniques developed, the TRF is often described as the "gold standard" method, despite its

475 disadvantages (Montpetit et al., 2014, Wang et al., 2018); it requires high amounts of DNA and is

476 labour-intensive and costly. The restriction enzymes used result in the inclusion of subtelomeric DNA,

477 which is contiguous to the telomere, thereby leading to a possible overestimation of TL. It is also unable

478 to detect short telomeres due to limited binding of the probe used for detection. In contrast, q-PCR-

479 based techniques are well suited for high-throughput analyses due to their simplicity and low costs.

480 The q-PCR-based techniques have, however, a primer dimerisation problem, which can be overcome

481 by choosing primers that bind to the C- and G-rich segments but are mismatched at the other bases

482 and by decreasing the temperature of the first cycles (Cawthon, 2009). However, the results from these

483 studies are limited in their ability to allow for comparisons between studies due to relatively high levels

484 of variation (Wang et al., 2018). The DNA extraction method, the storage conditions of the DNA,

485 telomere primer sequences, master mixes made by different vendors or homemade master mixes are

486 some examples of factors potentially impacting the assay (Martin-Ruiz et al., 2015, Lin et al., 2019).

487 Moreover, the use of conversion equations to determine TL in kb is the source of a higher degree of

488 bias in the TL values calculated by q-PCR techniques. Other attributes also warrant consideration, such

489 as the biological specimen to be evaluated. In the case of blood, which was analysed in the present

490 study, results reflect the lengths of the various blood cells that divide at different rates. Whereas

491 granulocytes (including neutrophils, eosinophils and basophils) have a lifespan of hours to days,

492 agranulocytes (including lymphocytes and monocytes) can have a lifespan of days to years (Montpetit

493 et al., 2014). Moreover, a different ratio of cell types could add variability and explain some of the

494 variations previously reported among different tissues (Lin et al., 2019, Morinha et al., 2020). As

495 concluded by a recent published international inter-calibration exercise (Martin-Ruiz et al., 2015),

496 there is a need for protocol homogenisation to allow comparisons of TL data obtained by different

497 laboratories in various published studies (Lai et al., 2018, Lin et al., 2019).

15

498   TL data obtained by q-PCR are still scarce in aquatic species. Izzo et al. (2010) reported TL values per
499   diploid genome between 86 and 590 kb in the muscle of the shark *Heterodontus portusjacksoni*, 12
500   and 585 kb in the muscle of carp *Cyprinus carpio* and 16 and 388 kb in the hind flipper biopsy of the
501   sea lion *Neophoca cinerea*, depending on the age.

502

4.2 Considering the influence of fish ontogenetic stage and sex on biomarker responses is of paramount importance

505   In the present study, it was initially decided to work only on fish from the same age and sex to take
506   into account the influences of these biotic factors on the measured chemical and biological markers.
507   Because age and sex could only be *a posteriori* established by otolith analysis and gonad examination,
508   respectively, the control over the sampling program was not total during the survey and the sampling
509   effort was significantly reduced afterward when constituting a subsample of fish from the same
510   ontogenetic stage and sex.

511   In flatfish, the response of classical biomarkers used in ecotoxicology and for biomonitoring purposes
512   varies with body length (used as a proxy of age) and sex. In dab from the Seine Estuary, DNA strand
513   breaks and 7-ethoxyresorufin-O-deethylase activity are influenced by both factors (Akcha et al., 2004,
514   Devier et al., 2013). Similar observations have been reported for the European flounder from the Baltic
515   Sea, concerning the response of other enzymatic biomarkers, namely the acetylcholinesterase and the
516   glutathione S-transferase activities (Napierska et al. 2005). These effects are likely related to the
517   existence in fish of differences with sex and age in their ability to bioaccumulate and biotransform
518   contaminants. For example, metal bioaccumulation (mercury, copper and zinc) depends on age in
519   several coastal fish species including the flounder; a normalisation technique was even recently
520   proposed to take this confounding factor into account and to allow reliable inter-site comparisons
521   (Suhareva et al., 2020). This is also the case for organic contaminants such as PCBs, for which
522   differences with sex have also been observed in several species, with higher concentrations expected
523   in males due to a higher energy expenditure rate (high resting metabolic rate and greater swimming
524   activity) compared to females (Mandenjian et al., 2016, Mandenjian, 2020). As a consequence, the
525   JAMP Guidelines for Contaminant-specific Biological Effects Monitoring (OSPAR Agreement Ref. No.
526   2008-09) highly recommended to consider the influences of these biotic factors when designing
527   sampling programs; therefore, monitoring should be performed during a relatively stable physiological
528   status and, in any case, during a period before spawning.

529   Concerning TL, the choice to analyse fish from the same age was particularly important due to the
530   highly probable ontogenetic effect on TL. Telomeres play a crucial role in protecting the chromosomes
531   at each cell cycle. This effect has already been investigated in different roundfish species with different

16

findings. Telomere shortening with age is not verified for all species, probably due to active telomerase activity and complex telomere dynamics in fish. In humans, telomerase expression in adults is restricted to germ line cells, stem cells and tumours (Cong et al., 2002); it is expressed in all tissues throughout the whole life of many fish species. This is also the case in the adult rainbow trout, *Oncorhynchus mykiss*, for which high telomerase activities were measured in all analysed tissues using the Telomerase Repeated Amplification Protocol (TRAP) assay, with the highest activities measured in the liver and the kidney (Klapper et al., 1998). Telomerase activity was also demonstrated by RTQ (real-time quantitative)-TRAP assay in the muscle of several species, such as the flounder (McChesney et al., 2005) and model laboratory fish such as the marine medaka, *Oryzias melastigma* (Peterson et al., 2015) and the zebrafish *Brachydanio rerio* (Anchelin et al., 2011). The way TL evolves with age appears to be different depending on the species. In the Atlantic Salmon *Salmo salar*, TL increased between embryo and larvae stage (McLennan et al., 2018) whereas it decreased between smolt and adult stages during a longitudinal study based on a recapture experiment that allowed TL measurement in the same individuals before and after migration (MacLennan et al., 2017). In the long-lived sturgeon *Acipenser baerii*, telomere shortening with age was also observed (Simide et al., 2016) whereas in the European seabass *Dicentrarchus labrax*, no correlation was observed between TL and age (Horn et al., 2008). It is noteworthy that for some species, such as the zebrafish, the way telomere length evolves with age seems to be directly dependent on the tissue type. By analysing the whole body, Anchelin et al. (2011) showed a non-linear age-related variation in TL, with an increase from larvae to adult stage and a significant telomere shortening in aged fish. By analysing different zebrafish tissues, Carneiro et al. (2016) showed that telomeres shorten to critical lengths with age only in specific tissues (e.g. gut, muscle), independently of their proliferation rate. To our knowledge, variation of TL with age has not yet been investigated in flatfish. There is, however, a strong interest in determining telomere shortening rates in these widely used sentinel species, as these data correlate to the lifespan in many birds and mammals (Whittemore et al., 2019).

In the present paper, no difference in TL was observed with sex. However, the number of samples was limited, requiring further confirmation. Different findings were reported in the bibliography concerning the influence of sex on TL in fish. In the common carp *Cyprinus carpio*, Izzo et al. (2014) showed no difference with sex or states of sexual maturity in muscle and fin clip telomere lengths. In contrast, sex differences in longevity and telomere length were observed in the marine medaka, both being higher in females than in males (Yip et al., 2017). In the females, the level of plasma E2 was shown to be positively correlated with TL. These results were consistent with the previous demonstration, in this species, of sex difference in telomerase activity (female > male) upon sexual maturation (Peterson et al., 2015).

17

4.3 Telomere length can vary under the influence of environmental factors such as chemical pollution

Telomere length is also under the influence of environmental factors such as chemical contamination, which can modify telomere dynamics and, as a consequence, the rate of telomere loss in fish. The chemical analyses performed in the present study showed that flounders from the Seine Estuary are exposed to mixtures of chemical contaminants, as previously reported in dab with the detection of PCBs, dioxins, furanes and PAHs in fish tissue and bile, respectively (Munschy et al., 2004, Devier et al., 2012), and in various vertebrate and invertebrate species for several historic and emerging contaminants (Tappin and Millward, 2015).

Exposure to these complex contaminant mixtures is responsible for a genotoxic stress in dab from the Seine Estuary (Akcha et al., 2003, 2004, Munschy et al., 2004, Devier et al., 2012). This could also be the case in flounders, presenting a similar level of DNA strand breaks. In fact, PAHs (Le Du-Lacoste et al., 2012), PCBs (Marabini et al., 2011), PBDEs (Sharma et al., 2018), OCPs and PFASs (Ayanda et al., 2018) are genotoxic in fish, which explains why in several fish species, correlations were previously observed between chemical body burden and level of DNA strand breaks. This is the case in dab from the Seine Estuary, for which correlations were observed with PAH metabolites, PCBs (∑PCBs and Σ7PCBs: CB-28, -52, -101, -118, -138, -153, -180) and PCDDs/PCDFs (Akcha et al., 2005, Devier et al., 2012). Correlations were also observed in the European flounder from the Baltic Sea when using lipid-based concentrations of PCB 118, Σ7PCB and Σm-oPCB (mono-ortho chlorinated congeners: CB-114, -118, -105, -156, -157, -167, -189) (Dabrovska et al., 2014) and in the Californian halibut *Paralichthys californicus* from Southern California bays and harbours with PAH metabolites (Brown and Steinert, 2003). In the present study, no correlation between chemical contamination and the level of % tail DNA was observed in flounders. The same observation was made for TL, which did not appear to be correlated with any of the contaminants measured in our study. Because we analysed a limited number of fish, all coming from the same area, this point requires further investigations, motivated by the positive correlations between relative TL and organochlorinated compounds (PCBs, DDT and OCPs), which could be observed when increasing the α risk value from 0.05 to 0.10. Telomeres are particularly sensitive to oxidative damage (Monaghan et al., 2018), which is induced by a wide range of environmental contaminants such as those measured in the present study (Valavanidis et al., 2006, Lushchak 2015). One reason for increased vulnerability is the presence of a high proportion of guanine bases in the telomeric sequence, which target oxyradicals (Honda et al., 2001, Kawanishi and Oikawa 2004). The underlying mechanisms of telomere loss by oxidative DNA lesions have been investigated

18

by several authors, who pointed out a replication fork collapse in the telomere region (e.g. Coluzzi et al., 2019).

The impact of chemical pollution on telomeres was mainly investigated in humans, with a high number of epidemiology and toxicology studies in the last decades. Based on the results, TL can be affected in different ways (decrease, increase or no effect), depending on e.g. the chemical contaminants studied, the mode of exposure and the type of cells analysed (Louzon et al., 2019, Ng and Amini, 2020). For example, exposure to PCBs and OCPs (as measured by their serum levels) was shown to impact leukocyte TL in humans (Karimi et al., 2020), whereas non-dioxin-like PCBs and dioxin-like PCBs (except for CB28) were related to increased TL; OCP exposure was related to telomere shortening. In another study focusing on children exposed to traffic-related air pollution, an inverse linear relationship was demonstrated between PAH level (daily individual exposure) and TL in peripheral blood mononuclear cells (Lee et al., 2017). Effects were also reported for PFASs for which prenatal exposure was associated with a significant decrease in leukocyte TL, but only in female new-borns (Liu et al., 2018). By using *in vitro* approaches, many contaminants were shown to interact with telomerase-related gene expression, telomerase activity and telomere shelterins, modifying telomere dynamics (Xin et al., 2016, Kahl et al., 2016, Ling et al., 2018). The same appears to be true for animals, particularly for birds, albeit with a more limited number of studies. In adult female black-legged kittiwakes *Rissa tridactyla*, a negative correlation was found between blood concentration of oxychlordane (major metabolites of chlordane-related contaminants) and TL (Blevin et al., 2016). The impact of PFASs was also investigated in this species, with different findings. In adults, no association could be determined between exposure to PFASs and absolute TL, with the exception of significantly elongated telomeres in birds presenting the highest concentration of PFASs (Blévin et al., 2017). In chicks of white-tailed eagles *Haliaeetus albicilla*, no relationship between the concentrations of organohalogenated compounds (PCBs, DDT, HCH, HCB: hexachlorobenzene) and TL was observed, despite significant changes in the antioxidant enzyme superoxide dismutase, plasma non-enzymatic antioxidant capacity and oxidative damage to plasma proteins (Sletten et al., 2016, Costantini et al., 2019). In contrast, in the adult glaucous gull *Larus hyperboreus*, some single PFAS compounds are positively correlated with the slowest rate of telomere shortening (Sebastiano et al., 2020). Similar to humans, the, contaminant effect on telomere dynamics in birds seems to vary according to the nature of the contaminant and the species. In flatfish, more investigations are needed to conclude on this point.

Similar to DNA strand breaks, telomere shortening in flounders could occur following oxyradical production related to contaminant exposure. As mentioned previously, DNA damage can contribute directly to telomere attrition due to replication fork collapse. Therefore, the absence of a relationship between these two types of genome damage can appear inconsistent. There could be, however, a bias

634 in the direct comparison of both markers, as changes in TL could be more integrative of a cumulative

635 damage produced by oxyradical attacks due to a more reduced repairing capacity than for DNA strand

636 breaks.

637 **5. Conclusion**

638 A protocol for TL measurement was adapted with success in the European flounder, widely used as

639 sentinel species in biomonitoring studies. It was then applied to a limited number of samples caught

640 in the Seine Estuary. In the absence of knowledge on the relationship between TL and age in this

641 species, fish age was determined in the laboratory by otolith sclerochronology to analyse only fish from

642 the same age, thereby limiting ontogenic variability among specimens. This requirement significantly

643 reduced the sampling effort, highlighting the necessity to increase fish catching in the field for this kind

644 of investigations, raising ethical and economic issues.

645 Because exposure to chemical contaminants could affect TL in flounder, we looked for correlations

646 with chemical body burden, which were not found. Due to the limited number of fish analysed and the

647 lack of knowledge on telomere dynamics in flatfish (e.g. age and sex effect, tissue effect, level of

648 telomerase activity), it is necessary to perform further investigations, motivated by the correlations

649 that were observed with organochlorinated compounds when decreasing statistical significance (α

650 value from 0.05 to 0.10). In addition to field studies based on several contrasted sites, it will be

651 particularly interesting to conduct controlled experiments at the laboratory for individual widely

652 distributed environmental contaminants and mixtures thereof. Determining the telomere shortening

653 rate following chemical stress could hence provide evidence of an impact of chemical pollution on the

654 lifespan of flatfish populations, as demonstrated for human and several animal species. Because

655 flatfish species can present differences in sensitivity to chemical pollutants, work should also be

656 conducted in more vulnerable species (e.g. *Solea solea*).

657

666

References

669 Akcha F., Hubert F., Pfhol-Leszkowicz A. (2003). Potential value of the comet assay and DNA adduct

670 measurement in dab (*Limanda limanda*) for assessment of *in situ* exposure to genotoxic compounds.

671 Mutat Res Gen Tox En 534: 21-32, DOI: 10.1016/S1383-5718(02)00244-9.

673 Akcha F., Leday G., Pfohl-Leszkowicz A. (2004). Measurement of DNA adducts and strand breaks in dab

674 (*Limanda limanda*) collected in the field: effects of biotic (age, sex) and abiotic (sampling site and

675 period) factors on the extent of DNA damage. Mutat Res Fund Mol M 552: 197-207, DOI:

676 10.1016/j.mrfmmm.2004.06.020.

678 Akcha F., Munschy C., Moisan K., Tronczynski J. (2005). Relation entre la contamination chimique de

679 l'Estuaire de la Seine et les effets génotoxiques et cancérigènes chez la limande. Ifremer,

680 R.INT.DCN/BE- 2005-08, pp 70.

682 Andrei R. C., Cristea V., Crețu M., Dediu L., Mogodan A. (2018). The effect of temperature on the

683 standard and routine metabolic rates of young of the year sterlet sturgeon (*Acipenser ruthenus*). AACL

684 Bioflux, 11: 1467-1475.

686 Auer S. K., Salin K., Anderson G. J., Metcalfe N. B. (2018). Individuals exhibit consistent differences in

687 their metabolic rates across changing thermal conditions. Comp Biochem Physiol A Mol Integr Physiol

688 217: 1–6, DOI: 10.1016/j.cbpa.2017.11.021.

690 Ayanda I. O., Yang M., Y. Zhang, Zha J. (2018). Cytotoxic and genotoxic effects of perfluorododecanoic

691 acid (PFDoA) in Japanese medaka. Knowl Manag Aquat Ecosyst 419: 9, DOI: 10.1051/kmae/2017058.

693 Axson E. L., Peterson K. E., Tellez-Rojo M. M., Goodrich J. M., Meeker J., Mercado-García A., Solano M.,

694 Needham B. L. (2018). Sex differences in telomere length are not mediated by sex steroid hormones

695 or body size in early adolescence. Gend Genome 2: 68-75, DOI: 10.1177/2470289718795177.

697 Barnes R. P., Fouquerel E., Opresko P. L. (2019). The impact of oxidative DNA damage and stress on

698 telomere homeostasis. Mech Ageing Dev 177: 37-45, DOI: 10.1016/j.mad.2018.03.013.

700 Barranger A., Akcha F., Rouxel J., Brizard R., Maurouard E., Pallud M., Menard D., Tapie N., Budzinski

701 H., Burgeot T., Benabdelmouna A. (2014). Study of genetic damage in the Japanese oyster induced by

21

702 an environmentally-relevant exposure to diuron: evidence of vertical transmission of DNA damage.

703 Aquat Toxicol 146: 93-104, DOI: 10.1016/j.aquatox.2013.10.032.

704

705 Blévin P., Angelier F., Tartu S., Ruault S., Bustamante P. (2016). Exposure to oxychlordane is associated

706 with shorter telomeres in arctic breeding kittiwakes. Sci Total Environ 563-564: 125-130, DOI:

707 10.1016/j.scititenv.2016.04.096.

708

709 Blévin P., Angelier F., Tartu S., Bustamante P., Herzke D., Moe B., Chastel O. (2017). Perfluorinated

710 substances and telomeres in an Arctic seabird: Cross-sectional and longitudinal approaches. Environ

711 Pollut 230: 360-367, DOI: 10.1016/j.envpol.2017.06.060.

712

713 Brown J. S. and Steinert S. A. (2003). DNA damage and biliary PAH metabolites in flatfish from Southern

714 California bays and harbors, and the Channel Islands. Ecol Indic 3: 263–274, DOI:

715 10.1016/j.ecolind.2003.11.004.

716

717 Bustin S. A., Benes V., Garson J. A., Hellemans J., Huggett J., Kubista M., Mueller R., Nolan T., Pfaffl M.

718 W., Shipley G. L., Vandesompele J., Wittwer C. T. (2009). The MIQE Guidelines: Minimum Information

719 for Publication of Quantitative Real-Time PCR Experiments. Clin Chem, 55: 611–622, DOI:

720 10.1373/clinchem.2008.112797.

721

722 Carneiro M. C., Henriques C. M., Nabais J., Ferreira T., Carvalho T., Ferreira M. G. (2016). Short

723 telomeres in key tissues initiate local and systemic aging in zebrafish. PLoS Genet 12: e1005798, DOI:

724 10.1371/journal.pgen.1005798.

725

726 Cawthon R. M. (2009). Telomere length measurement by a novel monochrome multiplex quantitative

727 PCR method. Nucleic Acids Res 37: e21, DOI: 10.1093/nar/gkn1027.

728

729 Coluzzi E., Leone S., Sgura A. (2019). Oxidative stress induces telomere dysfunction and senescence by

730 replication fork arrest. Cells 8: 19, DOI: 10.3390/cells8010019.

731

732 Cong Y-S., Wright W. E., Shay J. W. (2002). Human telomerase and its regulation. Microbiol Mol Biol R

733 66: 407-425, DOI: 10.1128/MMBR.66.3.407–425.2002.

734

22

735 Dabrowska H., Kopko O., Góra A., Waszak I., Walkusz-Miotk J. (2014). DNA damage, EROD activity, 736 condition indices, and their linkages with contaminants in female flounder (*Platichthys flesus*) from the 737 southern Baltic Sea. Sci Total Env 496 : 488-498, DOI:10.1016/j.scitotenv.2014.07.079.

738

739 Devier M-H., Le Du-Lacoste M., Akcha F., Morin B., Peluhet L., Le Menach K., Burgeot T., Budzinski H. 740 (2013). Biliary PAH metabolites, EROD activity and DNA damage in dab (*Limanda limanda*) from Seine 741 Estuary (France). Environ Sci Pollut Res 20: 708-722, DOI: 10.1007/s11356-012-1345-7.

742

743 Diopere E., Maes G. E., Komen H., Volckaert F. A. M., Groenen M. A. M. (2014). A genetic linkage map 744 of Sole (*Solea solea*): A tool for evolutionary and comparative analyses of exploited (flat)fishes. PLoS 745 One, 9: e115040, DOI: 10.1371/journal.pone.0115040.

746

747 Drevs T., Kadakas V., Lang T., Mellergaard S. (1999). Geographical variation in the age/length 748 relationship in Baltic flounder (*Platichthys flesus*). ICES J Mar Sci, 56: 134–137, DOI: 749 10.1006/jmsc.1999.0460.

750

751 Elmore L. W., Norris M. W., Sircar S., Bright A. T., McChesney P. A., Winn R. N., Holt S. E. (2008). 752 Upregulation of telomerase function during tissue regeneration. Exp Biol Med 233:958-67, DOI: 753 10.3181/0712-RM-345.

754

755 Flipo N., Lestel L., Labadie P., Meybeck M., Garnier J. (2020) Trajectories of the Seine River Basin. In: 756 The Handbook of Environmental Chemistry. Springer, Berlin, Heidelberg. 757 https://doi.org/10.1007/698_2019_437.

758

759 Foote C.G., Vleck D., Vleck C. M. (2013). Extent and variability of interstitial telomeric sequences and 760 their effects on estimates of telomere length. Mol Ecol Res 13: 417–428, DOI: 10.1111/1755-761 0998.12079.

762

763 Gardner M., Bann D., Wiley L., Cooper R., Hardy R., Nitsch D., Martin-Ruiz C., Shiels P., Sayer A. A., 764 Barbieri M., Bekaerth S., Bischoff C., Brooks-Wilson A. et al. (2014). Gender and telomere length: 765 Systematic review and meta-analysis. Exp Gerontol 51: 15-27, DOI: 10.1016/j.exger.2013.12.004

766

767 Harley C. B., Futcher A. B., Greider C. W. (1990). Telomeres shorten during ageing of human fibroblasts. 768 Nature 345: 458-460, DOI: 10.1038/345458a0.

769

770 Horn T., Gemmell N. J., Robertson B. C., Bridges C. R. (2008). Telomere length change in European sea

771 bass (*Dicentrarchus labrax*). Aust J Zool 56: 207–210, DOI: 10.1071/ZO08046.

772

773 Izzo C. (2010). Patterns of telomere length change with age in aquatic vertebrates and the phylogenetic

774 distribution of the pattern among jawed vertebrates. Thesis University of Adelaid School of Earth and

775 Environmental Science, http://hdl.handle.net/2440/63477.

776

777 Izzo C, Bertozzi T., Gillanders B., Donnellan S. (2014). Variation in telomere length of the common carp,

778 *Cyprinus carpio* (Cyprinidae), in relation to body length. Copeia 1: 87-94, DOI: 10.1643/CI-11-162.

779

780 Karimi B., Nodehib R. M., Yunesian M. (2020). Serum level of PCBs and OCPs and leukocyte telomere

781 length among adults in Tehran, Iran. Chemosphere 248: 126092, DOI:

782 10.1016/j.chemosphere.2020.126092

783

784 Kahl V. F. S., da Silva J., da Silvia F. R. (2016). Influence of exposure to pesticides on telomere length in

785 tobacco farmers: A biology system approach. Mutat Res Fund Mol 791-792: 19-26 DOI:

786 10.1016/j.mrfmmm.2016.08.003.

787

788 Lacaze E., Geffard O., Goyet D., Bony S., Devaux A. (2011). Linking genotoxic responses in *Gammarus*

789 *fossarum* germ cells with reproduction impairment, using the Comet assay. Environ Res 111: 626-634,

790 DOI: 10.1016/j.envres.2011.03.012.

791

792 Le Du-Lacoste M., Akcha F., Devier M-H., Morin B., Burgeot T., Budzinski H. (2013). Comparative study

793 of different exposure routes on the biotransformation and genotoxicity of PAHs in the flatfish species,

794 *Scophthalmus maximus*. Environ Sci Pollut Res 20: 690-707, DOI: 10.1007/s11356-012-1388-9.

795

796 Lee E. Y., Lin J., Noth E. M., Hammond S. K., Nadeau K. C., Eisen E. A., Balmes J. R. (2017). Traffic-related

797 air pollution and telomere length in children and adolescents living in Fresno, CA: A Pilot Study. J Occup

798 Environ Med 59: 446–452, DOI: 10.1097/JOM.0000000000000996.

799

800 Lei M., Zhang L., Lei J., Zong L., Li J., Wu Z., Wang Z. (2015). Overview of emerging contaminants and

801 associated human health effects. Biomed Res Int ID 404796, DOI: 10.1155/2015/404796.

802

803 Lejnine S., Makarov V. L., Langmore J. P. (1995). Conserved nucleoprotein structure at the ends of

804 vertebrate and invertebrate chromosomes. PNAS 92: 2393-2397, DOI: 10.1073/pnas.92.6.2393.

24

805

Ling X., Yang W., Zou P., Zhang G., Wang Z., Zhang X., Chen H., Peng K., Han F., Liu J., Cao J., Ao L. (2018). TERT regulates telomere-related senescence and apoptosis through DNA damage response in male germ cells exposed to BPDE *in vitro* and to B[a]P *in vivo*. Environ Pollut 235: 836-849, DOI: 10.1016/j.envpol.2017.12.099.

Liu H., Chen Q., Lei L., Zhou W., Huang L., Zhang J., Chen D. (2018). Prenatal exposure to perfluoroalkyl and polyfluoroalkyl substances affects leukocyte telomere length in female newborns. Environ Pollut 235: 446-452, DOI: 10.1016/j.envpol.2017.12.095.

Louzon M., Coeurdassier M., Gimbert F., Pauget B., de Vaufleury A. (2019). Telomere dynamic in humans and animals: Review and perspectives in environmental toxicology. Environ Int 131: 105025, DOI: 10.1016/j.envint.2019.105025

Lushchak V. I. (2015). Contaminant-induced oxidative stress in fish: a mechanistic approach. Fish Physiol Biochem 42: 711–747, DOI: 10.1007/s10695-015-0171-5.

Madenjian C. P., Rediske R. R., Krabbenhoft D. P., Stapanian M. A., Chernyak S. M., O'Keefe J. P. (2016). Sex differences in contaminant concentrations of fish: A synthesis. Biol Sex Differ 7:42, DOI: 10.1186/s13293-016-0090-x.

Madenjian C. P. (2020). Males exceeding females in whole fish polychlorinated biphenyl concentration mainly attributable to higher energy expenditure rate. Environ Toxicol Chem, 39: 951–952, DOI: 10.1002/etc.4685.

Marabini L., Calò R., Fucile S. (2011). Genotoxic effects of polychlorinated biphenyls (PCB 153, 138, 101, 118) in a fish cell line (RTG-2). Toxicol *in vitro*, 25:1045-1052, DOI: 10.1016/j.tiv.2011.04.004.

Martin-Ruiz C. M., Baird D., Roger L., Boukamp P., Krunic D., Cawthon R., Dokter M. M., van der Harst P., Bekaert S., de Meyer T., Roos G., Svenson U., Codd V., Samani N. J., McGlynn L., Shiels P. G., Pooley K. A., Dunning A. M., Cooper R., Wong A., Kingston A., von Zglinicki T. (2015). Reproducibility of telomere length assessment: an international collaborative study. Int J Epidemiol 44: 1673-83, DOI: 10.1093/ije/dyu191.

838

25

839 Mazéas O. and Budzinski H. (2005). Solid-phase extraction and purification for the quantification of

840 polycyclic aromatic hydrocarbon metabolites in fish bile. Anal Bioanal Chem 383:985-990,

841 DOI: 10.1007/s00216-005-0096-4.

842

843 McLennan D., Armstrong J. D., Stewart D. C., Mckelvey S., Boner W., Monaghan P., Metcalfe N. B.

844 (2017). Shorter juvenile telomere length is associated with higher survival to spawning in migratory

845 Atlantic salmon. Funct Ecol 31:2070–2079, DOI: 10.1111/1365-2435.12939.

846

847 McLennan D., Armstrong J. D., Stewart D. C., Mckelvey S., Boner W., Monaghan P., Metcalfe N. B.

848 (2018). Telomere elongation during early development is independent of environmental temperatures

849 in Atlantic salmon. J Exp Biol 221: jeb178616, DOI: 10.1242/jeb.178616.

850

851 McChesney P. A., Elmore L. W., Holt S. E. (2005). Vertebrate Marine Species as Model Systems for

852 Studying Telomeres and Telomerase. Zebrafish 1: 349-355, DOI: 10.1089/zeb.2005.1.349.

853

854 Molbert N., Angelier F., Alliot F., Ribout C., Goutte A. (2021). Fish from urban rivers and with high

855 pollutant levels have shorter telomeres. Biology Letters **17 :** 20200819-20200819 , DOI:

856 10.1098/rsbl.2020.0819

857

858 Møller P., Wils R. S., Jensen D. M., Andersen M. H. G., Roursgaard M. (2018). Telomere dynamics and

859 cellular senescence: an emerging field in environmental and occupational toxicology. Crit Rev Toxicol

860 48: 767-788, DOI: 10.1080/10408444.2018.1538201.

861

862 Monaghan P., Eisenberg D. T. A., Harrington L., Nussey D. (2018). Understanding diversity in telomere

863 dynamics. Philos Trans R Soc Lond B Biol Sci 373: 20160435, DOI: 10.1098/rstb.2016.0435.

864

865 Monaghan P. and Ozanne S. E. (2018). Somatic growth and telomere dynamics in vertebrates:

866 Relationships, mechanisms and consequences. Philos Trans R Soc Lond B Biol Sci 373: 20160446, DOI:

867 10.1098/rstb.2016.0446.

868

869 Montpetit A., Alhareeri A., Montpetit M., Starkweather A., Elmore L., Filler K., Mohanraj L., Burton C.,

870 Menzies V., Lyon D., Jackson-Cook C. (2014). Telomere length: a review of methods for measurement.

871 Nurs Res 63: 289–299, DOI: 10.1097/NNR.0000000000000037.

872

873 Morinha F., Magalhães P., Blanco G. (2020). Standard guidelines for the publication of telomere qPCR

874 results in evolutionary ecology. Mol Ecol Res 20: 635-648, DOI: 10.1111/1755-0998.13152.

875

876 Munschy C., Vigneau E., Bely N., Héas-Moisan K., Olivier N., Pollono C., Hollanda S., Bodin N. (2020a).

877 Legacy and emerging organic contaminants: levels and profiles in top predator fish from the western

878 Indian Ocean in relation to their trophic ecology. Environ Res 188 :109761, DOI:

879 10.1016/j.envres.2020.109761.

880

881 Munschy C., Bely N., Héas-Moisan K., Olivier N., Pollono C., Hollanda S., Bodin N. (2020b). Tissue-

882 specific bioaccumulation of a wide range of legacy and emerging persistent organic contaminants in

883 swordfish (*Xiphias gladius*) from Seychelles, Western Indian Ocean. Mar Pollut Bull 158: 111436, DOI:

884 10.1016/j.marpolbul.2020.111436.

885

886 Ng C. Y. and Amini F. (2020). Telomere length alterations in occupational toxicants exposure: an

887 integrated review of the literature. Expo Health, DOI: 10.1007/s12403-020-00367-4.

888

889 O'Callaghan N. J., Dhillon V. S., Thomas P., Fenech M. (2008). A quantitative real-time PCR method for

890 absolute telomere length. Biotechniques 44: 807-809, DOI: 10.2144/000112761.

891

892 Ocalewicz K. (2013). Telomeres in Fishes. Cytogenet Genome Res 141: 114-125, DOI:

893 10.1159/000354278. DOI 10.1159/000354278.

894

895 Panfili J., De Pontual H., Troadec H., Wrigh P. J. (2002). Manual of fish sclerochronology. Ifremer/IRD

896 Coedition, Brest, France.

897

898 Pauliny A., Devlin R. H., Johnsson J. I., Blomqvist D. (2015). Rapid growth accelerates telomere attrition

899 in a transgenic fish. BMC Evol Biol, 15:159, DOI: 10.1186/s12862-015-0436-8.

900

901 Peterson D. R., Oi Lam Mok H., Wai Ting Au D. (2015). Modulation of telomerase activity in fish muscle

902 by biological and environmental factors. Comp Biochem Physiol C Toxicol Pharmacol 178: 51-59, DOI:

903 10.1016/j.cbpc.2015.09.004.

904

905 Pflaff M. W. (2004). Quantification strategies in real-time PCR. In S.A Bustin (Ed.), A-Z of quantitative

906 PCR, pp. 87–120. La Jolla, CA: IUL Biotechnology Series, International University Line.

907

908 Remen M., Nederlof M. A. J., Folkedal O., Thorsheim G., Sitjà-Bobadilla A., Pérez-Sánchez J., Oppedal
909 F., Olsen R. E. (2015). Effect of temperature on the metabolism, behaviour and oxygen requirements
910 of Sparus aurata. Aquacult Environ Interact, 7:115-123, DOI 10.3354/aei00141.

911

912 Saygun S (2015). The first karyological description of European Flounder, *Platichthys flesus luscus*
913 (Pallas, 1814) (Pisces, Pleuronectiformes) living in the Black Sea. EgeJFAS, 32: 9-14, DOI:
914 10.12714/egejfas.2015.32.1.02.

915

916 Sebastiano M., Angelier F., Blévin P., Ribout C., Sagerup K., Descamps S., Herzke D., Moe B., Barbraud
917 C., Bustnes J. O., Gabrielsen G. W., Chastel O. (2020). Exposure to PFAS is Associated with Telomere
918 Length Dynamics and Demographic Responses of an Arctic Top Predator. Env Sci Tech Article ASAP
919 DOI: 10.1021/acs.est.0c03099.

920

921 Sharma P., Chadha P., Singh Saini H. (2018). Tetrabromobisphenol A induced oxidative stress and
922 genotoxicity in fish *Channa punctatus*. Drug Chem Toxicol 42: 559-564, DOI:
923 10.1080/01480545.2018.1441864.

924

925 Simide R., Angelier F., Gaillard S., Stier A. (2016). Age and Heat Stress as Determinants of Telomere
926 Length in a Long-Lived Fish, the Siberian Sturgeon. Physiol Biochem Zool 89: 441-447, DOI:
927 10.1086/687378.

928

929 Suhareva, N., Aigars, J., Poikane, R., & Jansons, M. (2020). Development of fish age normalization
930 technique for pollution assessment of marine ecosystem, based on concentrations of mercury, copper,
931 and zinc in dorsal muscles of fish. Environ Monit Assess, 5: 192-279, DOI: 10.1007/s10661-020-08261-
932 x.

933

934 Tappin, A. D., and Millward, G. E. (2015). The English Channel: Contamination status of its transitional
935 and coastal waters. Mar Pollut Bull, 95: 529–550, DOI: 10.1016/j.marpolbul.2014.12.012.

936

937 Lai T-P., Wright W. E., Shay J. W. (2018). Comparison of telomere length measurement methods. Phil
938 Trans R Soc B 373: 20160451, DOI: 10.1098/rstb.2016.0451.

939

940 U.S. Environmental Protection Agency (1998) Method 7473 (SW-846): Mercury in solids and solutions
941 by thermal decomposition, amalgamation, and atomic absorption spectrophotometry, Revision 0.

942

943 van der Hammen T. and Poos J. J. (2012). Data evaluation of data-limited stocks: dab, flounder, witch, lemon sole, brill, turbot and horse mackerel. Institute for Marine Resources and Ecosystem Studies (IMARES), Wageningen. Report No. C110/12.

944

947 Vitale, F., Worsøe Clausen L., Ní Chonchúir G. (2019) (Eds). Handbook of fish age estimation protocols and validation methods. ICES Cooperative Research Report No. 346. 180 pp., DOI: 10.17895/ices.pub.5221.

950

951 Wang Y., Savage SA., Alsaggaf R., Aubert G., Dagnall G. L., Spellman S. R., Lee S. J., Hicks B., Jones K., Katki H. A., Gadalla S. M. (2018). Telomere length calibration from qPCR measurement: limitations of current method. Cells 7: 183, DOI:10.3390/cells7110183.

954

955 Wessel N., Rousseau, S., Caisey X., Quiniou F., Akcha F. (2007). Investigating the relationship between embryotoxic and genotoxic effects of benzo[alpha]pyrene, 17 alpha-ethinylestradiol and endosulfan on *Crassostrea gigas* embryos . Aquat Toxicol 85: 133-142, DOI: 10.1016/j.aquatox.2007.08.007.

958

959 Wessel N., Le Dû-Lacoste M., Budzinski H., Burgeot T., Akcha F. (2013). UPLC MS/MS quantification of primary metabolites of benzo[a]pyrene and fluoranthene produced in vitro by Sole (*Solea solea*) liver microsomal activation, Polycycl Aromat Compd 33: 52-71, DOI: 10.1080/10406638.2012.725197.

962

963 Whittemore, Elsa Vera, Eva Martínez-Nevado, Carola Sanpera, and Maria A. Blasco (2019). Telomere shortening rate predicts species life span. PNAS 116: 15122-15127, DOI: 10.1073/pnas.1902452116.

965

966 Xin X., Senthilkumar P. K., Schnoor J. L., Ludewig G. (2016). Effects of PCB126 and PCB153 on telomerase activity and telomere length in undifferentiated and differentiated HL-60 cells. Environ Sci Pollut Res Int 23: 2173–2185, DOI: 10.1007/s11356-015-5187-y.

969

970 Yip B. W. P., Mok H. O. L., Peterson D. R., Wan M. T., Taniguchi Y., Ge W., Au D. W. T. (2017). Sex-dependent telomere shortening, telomerase activity and oxidative damage in marine medaka *Oryzias melastigma* during aging. Mar Pollut Bull 124: 701–709, DOI: 10.1016/j.marpolbul.2017.01.021.

973

974 Zglinicki T. (2002). Oxidative stress shortens telomeres. Trends Biochem Sci 27: 339-344, DOI: 10.1016/s0968-0004(02)02110-2.

976

977 Zhao F., Wang B., Zhang X. (2015). Induction of DNA base damage and strand breaks in peripheral 978 erythrocytes and the underlying mechanism in goldfish (*Carassius auratus*) exposed to 979 monocrotophos. Fish Physiol Biochem 41: 613-624, DOI: 10.1007/s10695-015-0032-2.

980

981

1
2
3
4
5
6
7
8
9
10
11
12
13
14
15
16
17
18
19
20
21
22
23
24
25
26
27
28
29
30
31
32
33
34
35
36
37
38
39
40
41
42
43
44
45
46
47
48
49
50
51
52
53
54
55
56
57
58
59
60
61
62
63
64
65

Tables

Table 1: Validated primer set composition and concentrations for the amplification of telomeric sequence and reference gene in flounder

Sequence/ gene	GeneBank number (NCBI)	Sens	5'-3' Sequence	Concentration nM
GAPDH	KJ510524.1	Forward	CCT-GCC-GTC-ACT-GGG-ATT-AC	500
		Reverse	ACA-GCT-CTC-CCA-CTC-TCC-TC	500
Telomere	(O'Callaghan et al., 2008)	Forward	CGG-TTT-GTT-TGG-GTT-TGG-GTT-TGGGTT-TGG-GTT-TGG-GTT	200
		Reverse	GGC-TTG-CCT-TAC-CCT-TAC-CCT-TACCCT-TAC-CCT-TAC-CCT	450

Table 2: q-PCR efficiency of the different set of primers used for the measurement of TL.

Primer set	Type of samples	Efficiency (%)	Coefficient of determination (R^2)
GAPDH	Composite flounder DNA	104	0.99
	GAPDH oligomer	99	0.99
Telomeres	Composite flounder DNA	103	0.98
	Telomere oligomer	98	0.97

Table 3: Liver metal concentrations (n=8, mean ± standard deviation, mg kg^{-1} dw) in flounders from Seine Estuary.

	Ag	As	Cd	Co	Cu	Fe
Liver	0.35 ± 0.22	16.89 ± 5.40	0.19 ± 0.07	0.26 ± 0.12	46.77 ± 10.73	170.5 ± 66.7
	Hg	Mn	Mo	Pb	Zn	Σ
	0.13 ± 0.05	2.98 ± 0.98	0.31 ± 0.07	0.09 ± 0.06	105.3 ± 16.1	343.9 ± 87.8

	Hg
Muscle	0.270 ± 0.065

Table 4: Concentrations (ng g^{-1} dw) of PCBs (∑ 8 congeners), DDTs (∑ 5 isomers), HCHs (∑ 3 isomers), dieldrin, PBDEs (∑ 8 congeners), PFOS and PFCAs (∑ 7 compounds with the carbon chain length > C8) in flounder muscle collected in ES (n=8, mean ± standard deviation).

PCBs	DDTs	HCHs	Dieldrin
97.2 ± 25.3	2.20 ± 0.58	0.05 ± 0.01	0.31 ± 0.07

PBDEs	PFOS	PFCAs
0.51 ± 0.14	3.47 ± 1.20	1.37 ± 0.34

Table 5: Correlation matrix between absolute and relative TL, DNA damage and chemical contaminant concentrations in the flounder (N= 8, R^2: coefficient of determination, p value is given for α = 0.05, underlined values are significant for α = 0.10)

	Absolute TL		Relative TL		% Tail DNA	
	R^2	p value	R^2	p value	R^2	p value
% Tail DNA	0.167	0.315	0.305	0.156	-	-
PAH metabolites	0.070	0.525	0.235	0.223	0.217	0.245
TMEs	0.090	0.470	0.067	0.535	0.236	0.222
PCBs	0.327	0.139	0.382	<u>0.103</u>	0.199	0.268
DDT	0.374	0.107	0.423	<u>0.081</u>	0.295	0.164
HCH	0.022	0.726	0.049	0.598	0.025	0.711
Dieldrin	0.335	0.133	0.349	0.123	0.167	0.314
PFOS	0.050	0.594	0.042	0.626	0.137	0.368
PFCA	0.123	0.395	0.100	0.445	0.031	0.678
OCPs	0.368	0.111	0.414	<u>0.085</u>	0.278	0.179
PBDEs	0.184	0.290	0.219	0.242	0.186	0.286
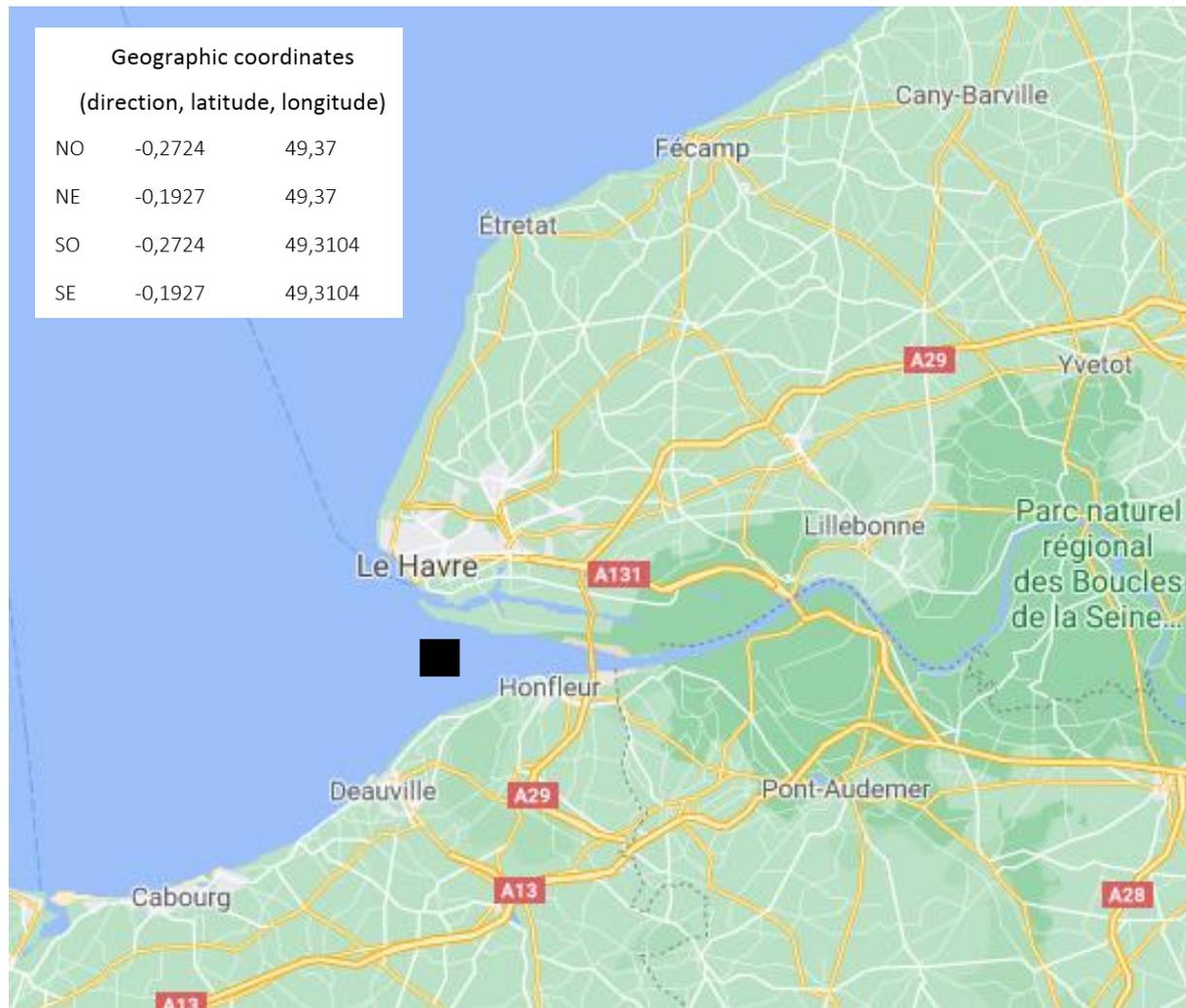
Figure 1: Localization of the sampling location in Seine Bay where flounders were caught during the SeliSeine survey (13-21 September 2018, R/V Antéa)
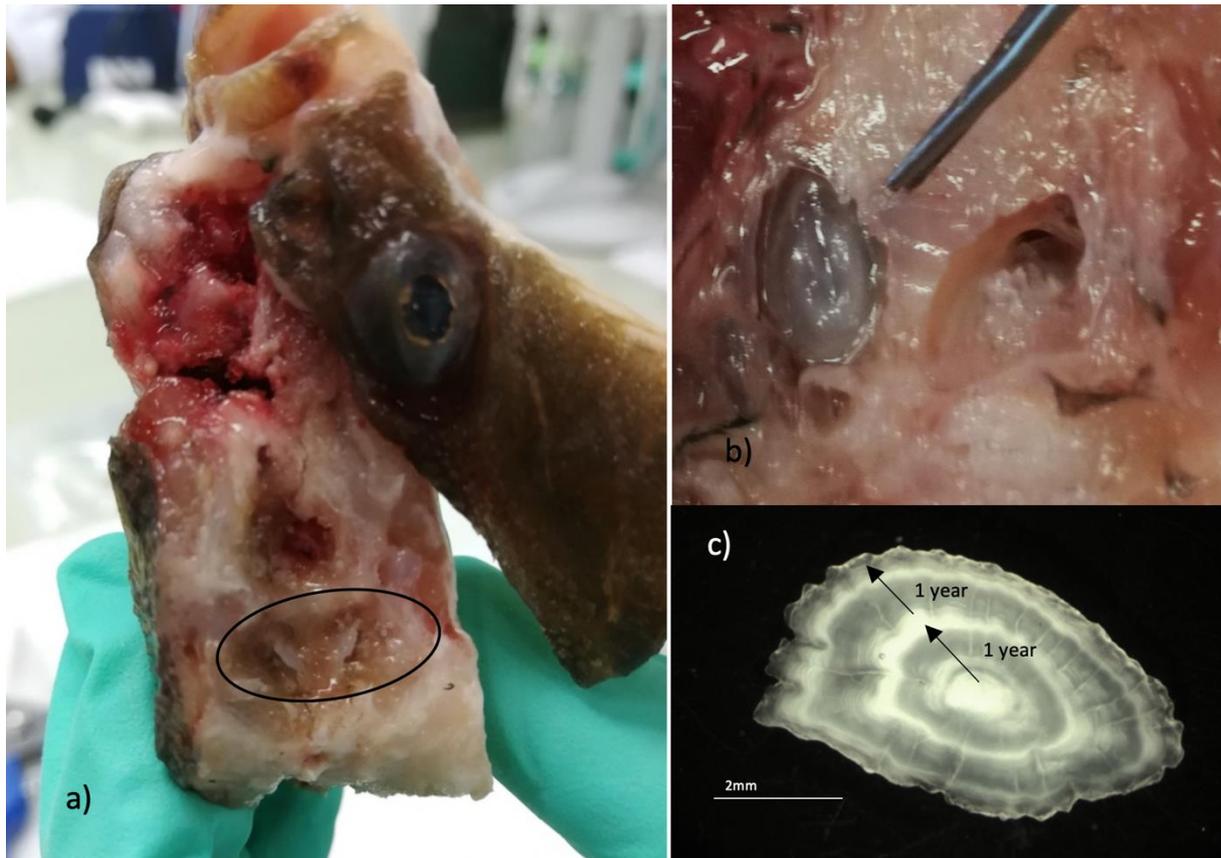
Figure 2: Sampling of flounder otoliths. After opening the skull (a), the sagittal otoliths are in the inner ear (b). The whole otolith are analysed under a microscope (c). The annual growth ring (i.e. annulus) counted on otoliths were represented by alternations of an opaque and a hyaline zone (here, a 2-year-old flounder).
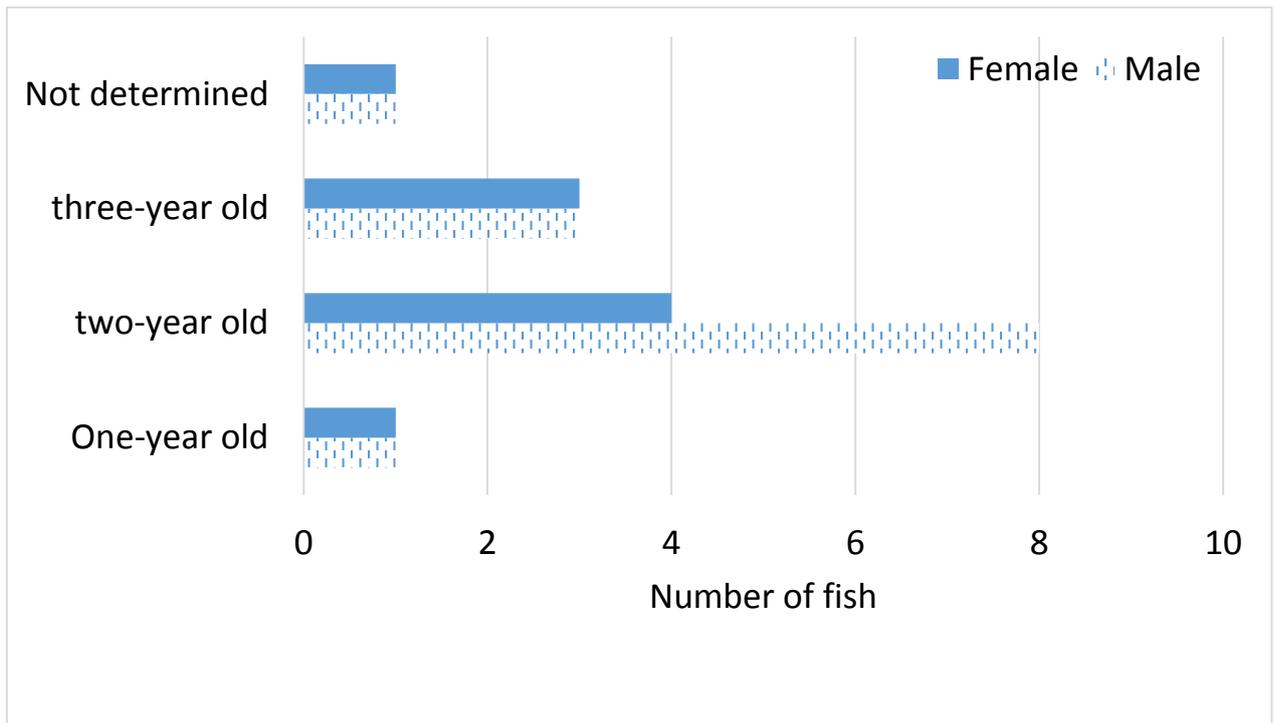
Figure 3: Number and sex of flounders caught during the survey. Not determined: the sclerochronology analysis could not be carried out because of the physical state of the otoliths being either broken or decalcified.
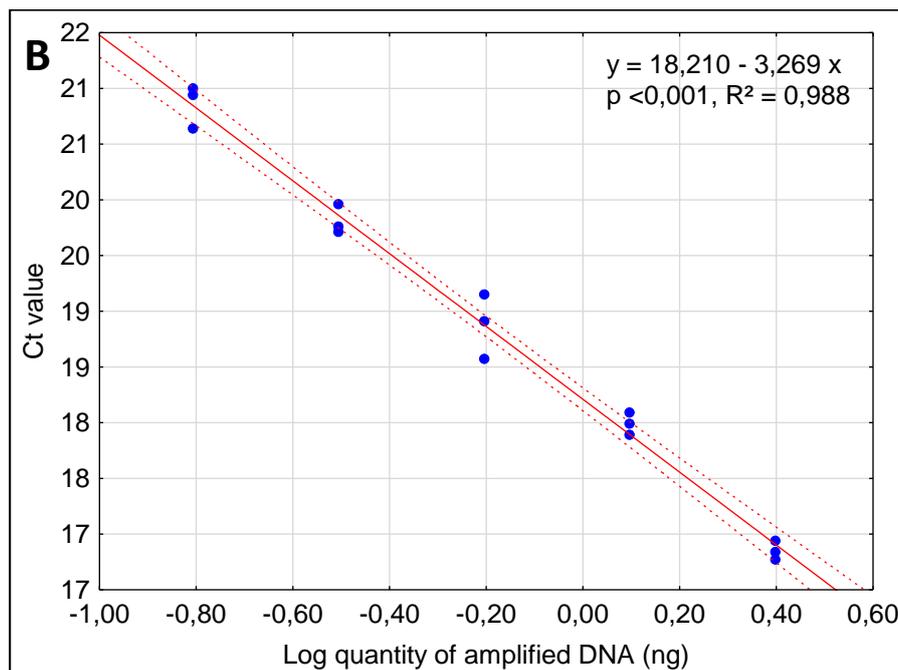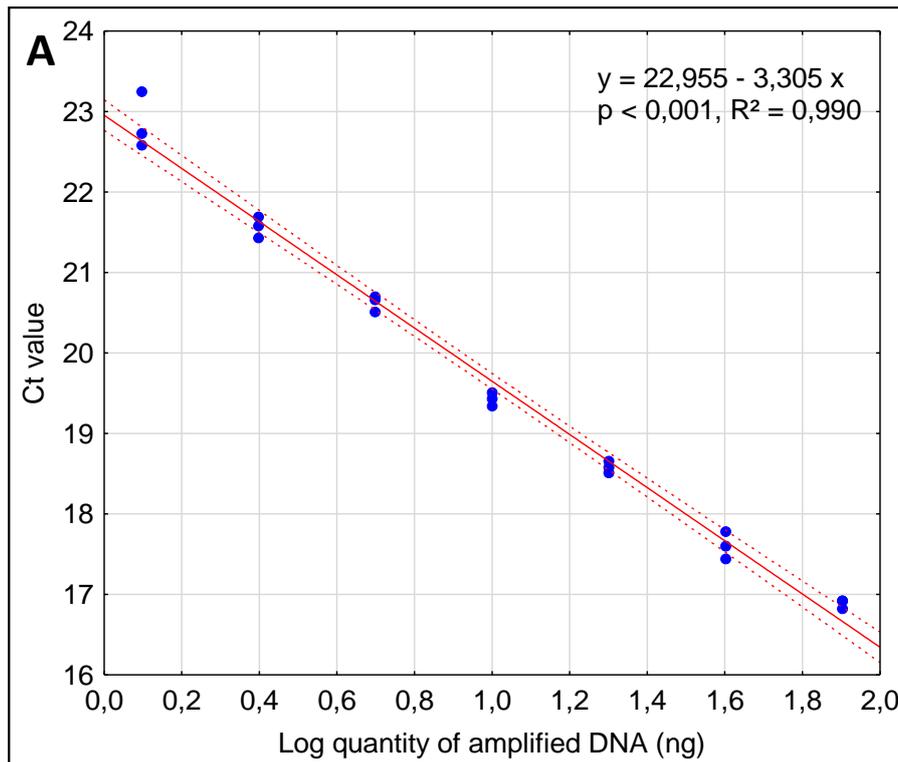
Figure 4: Validation of the q-PCR conditions by the linear relationship between amplified DNA amount and Ct values for (A) GAPDH gene and (B) telomeres. Regression bands represented the 95% confidence interval.
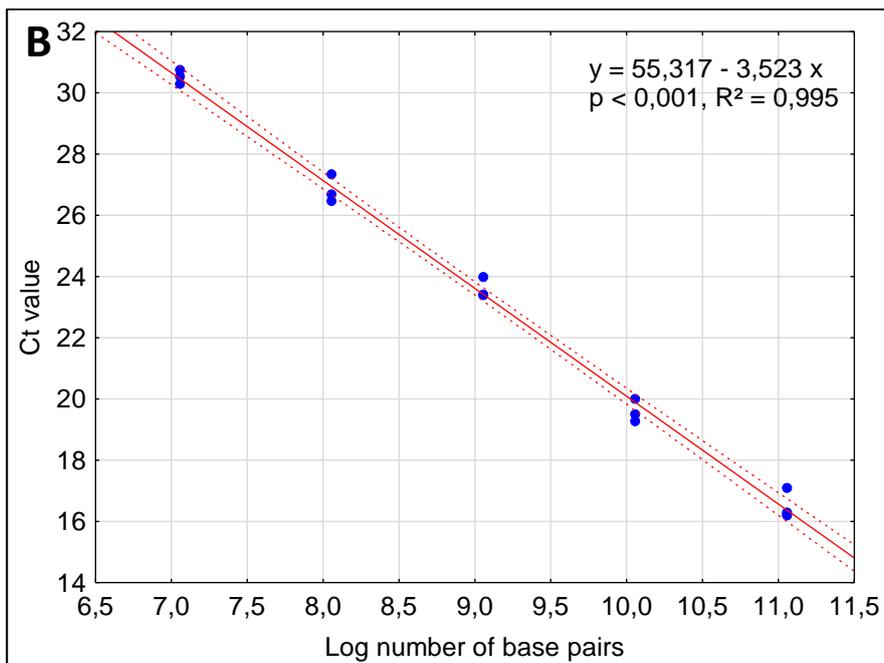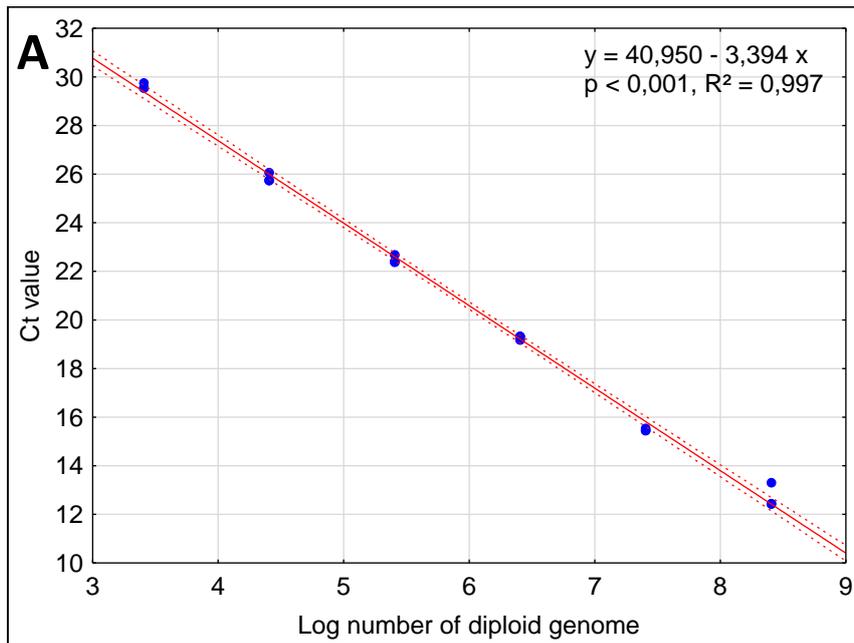
Figure 5: Calibration curve established for (A) GAPDH oligomer and (B) telomeric oligomer. For each calibration curve, plasmidic DNA was added to maintain the amount of DNA stable (1ng) in each well of the plate. Regression bands represented the 95% confidence interval.
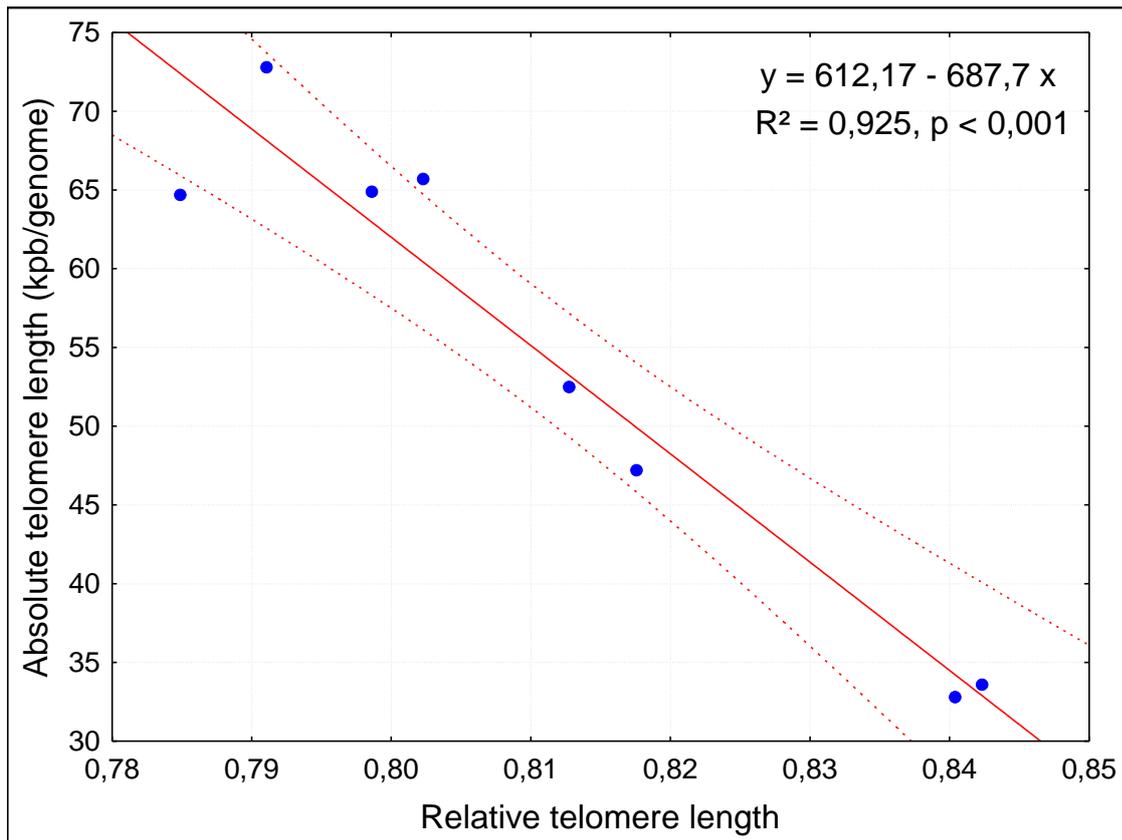
Figure 6: Correlation between absolute and relative TLs in the European flounder. Regression bands represented the 95% confidence interval.

CRediT author statement

F. Akcha: conceptualisation, methodology, writing-original draft preparation, funding acquisition, C. Cahuc: methodology, validation, J. Rouxel: methodology, C. Munschy: analysis of organic contaminants, Y. Aminot: analysis of organic contaminants, T. Chouvelon: analysis of MTEs, K. Mahe: analysis of fish otoliths, H. Budzinski: analysis of PAH metabolites, A. Mauffret: resources, funding acquisition.

Author Competing Interests

Funding Sources: Financial support for research (salaries, equipment, supplies, travel reimbursement), speaker/organizer honoraria.

Employment: Employment while engaged in this research, present or anticipated employment by any organization that may gain or lose financially through publication of this paper.

Personal Financial Interests: Stocks or shares in or ownership of companies affected by publication of this research, consulting fees/remuneration, royalties, from organizations which may profit or lose as a result of publication, patents or patient applications whose value and integrity may be affected due to publication.

Institutional Competing Interests

Are you aware that your academic institution or employment has a financial interest in or a financial conflict with the subject matter or materials discussed in this manuscript? Yes/**No**

<div align="center">

DECLARATION OF COMPETING INTERESTS

</div>

Title of Manuscript:
Measurement of telomere length in the European flounder (*Platichthys flesus*) from the Seine Estuary: investigating a link between telomere length, DNA damage and chemical body burden

Corresponding Author:
Farida AKCHA

None declared under financial, general, and institutional competing interests. I had full access to all study data, take fully responsibility for the accuracy of the data analysis, and have authority over manuscript preparation and decisions to submit the manuscript for publication.

F. Akcha

5th January 2021